JGR Oceans

RESEARCH ARTICLE
10.1029/2020JC016930

Arctic Ocean Freshwater in CMIP6 Ensembles: Declining Sea Ice, Increasing Ocean Storage and Export

Hannah Zanowski[1], Alexandra Jahn[1], and Marika M. Holland[2]

[1]Department of Atmospheric and Oceanic Sciences and Institute of Arctic and Alpine Research, University of Colorado Boulder, Boulder, CO, USA, [2]National Center for Atmospheric Research, Boulder, CO, USA

Abstract The Arctic has undergone dramatic changes in sea ice cover and the hydrologic cycle, both of which strongly impact the freshwater storage in, and export from, the Arctic Ocean. Here we analyze Arctic freshwater storage and fluxes in seven climate models from the Coupled Model Intercomparison Project Phase 6 (CMIP6) and assess their performance over the historical period (1980–2000) and in two future emissions scenarios, SSP1-2.6 and SSP5-8.5. Similar to CMIP5, substantial differences exist between the models' Arctic mean states and the magnitude of their 21st century storage and flux changes. In the historical simulation, most models disagree with observations over 1980–2000. In both future scenarios, the models show an increase in liquid freshwater storage and a reduction in solid storage and fluxes through the major Arctic gateways (Bering Strait, Fram Strait, Davis Strait, and the Barents Sea Opening) that is typically larger for SSP5-8.5 than SSP1-2.6. The liquid fluxes are driven by both volume and salinity changes, with models exhibiting a change in sign (relative to 1980–2000) of the freshwater flux through the Barents Sea Opening by mid-century, little change in the Bering Strait flux, and increased export from the remaining straits by the end of the 21st century. In the straits west of Greenland (Nares, Barrow, and Davis straits), the models disagree on the behavior of the liquid freshwater export in the early-to-mid 21st century due to differences in the magnitude and timing of a simulated decrease in the volume flux.

Plain Language Summary The Arctic Ocean has changed dramatically due to melting sea ice and increasing river water input and rain- and snowfall. Keeping track of these sources of freshwater helps us understand how the Arctic Ocean is changing and how it will change in the future. In this study, we use several state-of-the-art climate models to understand these freshwater changes by calculating the amount of freshwater stored in, and transported in and out of, the Arctic Ocean. We first compare the models' freshwater values to observations and then determine how these values have changed at the end of the 21st century. We find that most models do not agree well with observations, and large differences in the size of the freshwater storage and transport also exist between them. Despite these differences, all models show that freshwater stored in and transported by sea ice decreases strongly by the end of the 21st century, while freshwater stored in the Arctic Ocean increases as well as freshwater transported out of the Arctic Ocean in most places. These changes indicate that by the end of this century the Arctic Ocean will be very different than it is today.

Key Points:

- Historical Arctic freshwater storage and fluxes vary widely across a subset of CMIP6 models and few are consistently close to observations
- Projections show declining solid and increasing liquid freshwater storage and fluxes in agreement with previous CMIP studies
- Large uncertainty exists in projections of liquid freshwater fluxes west of Greenland due to model differences in simulated velocities

Supporting Information:

Supporting Information may be found in the online version of this article.

Correspondence to:

H. Zanowski,
hannah.zanowski@colorado.edu

Citation:

Zanowski, H., Jahn, A., & Holland, M. M. (2021). Arctic Ocean freshwater in CMIP6 ensembles: Declining sea ice, increasing ocean storage and export. *Journal of Geophysical Research: Oceans*, *126*, e2020JC016930. https://doi.org/10.1029/2020JC016930

Received 30 OCT 2020
Accepted 13 MAR 2021

Author Contributions:

Conceptualization: Alexandra Jahn, Marika M. Holland
Funding acquisition: Alexandra Jahn, Marika M. Holland
Investigation: Hannah Zanowski
Methodology: Hannah Zanowski
Supervision: Alexandra Jahn
Visualization: Hannah Zanowski
Writing – original draft: Hannah Zanowski, Alexandra Jahn
Writing – review & editing: Hannah Zanowski, Alexandra Jahn, Marika M. Holland

1. Introduction

The Arctic Ocean freshwater system is undergoing rapid change. Arctic sea ice is declining (Stroeve et al., 2007, 2012), the Greenland ice sheet is melting (e.g., Shepherd et al., 2020), permafrost is thawing (e.g., Biskaborn et al., 2019; Rowland et al., 2010), and river discharge (e.g., Peterson et al., 2002, 2006) and precipitation are increasing (e.g., Rawlins et al., 2010), all pointing to an acceleration of the Arctic freshwater cycle. As a result of these changes, liquid (oceanic) freshwater storage has increased over the past few decades while solid (sea ice) storage has decreased (Giles et al., 2012; Haine et al., 2015; Proshutinsky et al., 2009; Rabe et al., 2011, 2014; Wang et al., 2018, 2019). With the exception of the liquid freshwater flux through Bering Strait (Woodgate, 2018; Woodgate et al., 2012), trends in the liquid and solid freshwater fluxes through the remaining Arctic gateways (Fram Strait, the Barents Sea Opening, and straits in the Canadian Arctic Archipelago) have not been detected (e.g., Beszczynska-Möller et al., 2011; Curry et al., 2011, 2014; de Steur et al., 2009, 2018; Haine et al., 2015), although we might expect to see such trends in the coming decades (Jahn & Laiho, 2020). These changes in Arctic freshwater have major implications for the Arctic, but they are also of global relevance (Prowse et al., 2015). The fluxes through Fram and Davis

straits and the Barents Sea Opening directly interact with the North Atlantic, potentially impacting North Atlantic Deep Water (NADW) formation and the Atlantic Meridional Overturning Circulation (AMOC) (Jahn & Holland, 2013; Sévellec et al., 2017; Thornalley et al., 2018; Yang et al., 2016). Great Salinity Anomalies (e.g., Belkin et al., 1998; Dickson et al., 1988) have occurred periodically in the North Atlantic due to Beaufort Gyre freshwater release, and liquid fluxes through the Fram Strait impact the North Atlantic (e.g., de Steur et al., 2009, 2018). In turn, North Atlantic variations also feed back onto the Arctic, leading to further change. One notable example of this is the "Atlantification" (Polyakov et al., 2017) of the Barents Sea, which has been found to limit the extent of winter sea ice there (Barton et al., 2018).

Many modeling studies have attempted to elucidate the dynamics and impacts (both local and global) of changing Arctic freshwater storage and fluxes (e.g., Aksenov et al., 2010; Condron et al., 2009; Cornish et al., 2020; Häkkinen & Proshutinsky, 2004; Holland et al., 2006, 2007; Jahn & Holland, 2013; Jahn & Laiho, 2020; Jahn et al., 2010; Koenigk et al., 2007; Lique et al., 2016; McGeehan & Maslowski, 2012; Shu et al., 2018; Wang et al., 2016a, 2016b, 2019). Model intercomparison studies such as the Arctic Ocean Model Intercomparison Project (AOMIP; Proshutinsky et al., 2011), the Forum for Arctic Modeling and Observational Synthesis (FAMOS; Proshutinsky et al., 2016), the Coordinated Ocean-ice Reference Experiments (COREs; Griffies et al., 2009), and previous Coupled Model Intercomparison Projects (CMIP3 and CMIP5; Meehl et al., 2007; Taylor et al., 2012) have been critical for improving our understanding of the Arctic freshwater system and its future changes. Although simulation of the Arctic freshwater system improved in CMIP5 relative to CMIP3 (Shu et al., 2018), studies using both CMIP3 (Holland et al., 2007; Hu & Myers, 2014; Kattsov et al., 2007; Koenigk et al., 2007) and CMIP5 (Jahn & Laiho, 2020; Shu et al., 2018; Vavrus et al., 2012) models consistently project increased liquid storage and export and decreased solid storage and export over the 21st century, suggesting that the models can robustly simulate forced trends. However, intermodel differences remain large (Jahn et al., 2012; Shu et al., 2018; Wang et al., 2016a, 2016b), and in CMIP5 some models still did not have open gateways west of Greenland (Shu et al., 2018). With the next generation of models from the Coupled Model Intercomparison Project Phase 6 (CMIP6; Eyring et al., 2016) now available, whether or not these new models show improvements is an open question.

Here, we analyze 20th and 21st century Arctic Ocean solid and liquid freshwater storage and fluxes in a subset of models from CMIP6. We assess the performance of their historical simulations compared to late 20th century observations and compare their 21st century projections in two future emissions scenarios (O'Neill et al., 2016) from ScenarioMIP, SSP1-2.6 (low emissions) and SSP5-8.5 (high emissions). We find that freshwater storage and fluxes still vary widely across models, and few are consistently close to observations. The former result holds for the future scenarios as well, although the models generally agree that solid storage and fluxes will decrease while liquid storage and fluxes will increase, in agreement with previous CMIP generations. As an improvement over CMIP5, all models analyzed here have two gateways west of Greenland, allowing for the first time a CMIP comparison of the fluxes through the Nares and Barrow straits.

2. Methods

2.1. Freshwater Storage, Column, and Flux Definitions

Solid (sea ice and snow) and liquid (ocean) freshwater storage are computed for the Arctic Ocean as defined by the boundaries of the Bering, Davis, and Fram Straits and the Barents Sea Opening (Figure 1h; dark red lines). Freshwater fluxes are computed through these straits as well as the Nares and Barrow straits in the Canadian Arctic Archipelago (Figure 1h; orange lines). As in previous observational and modeling studies (e.g., Aagaard & Carmack, 1989; Haine et al., 2015; Holland et al., 2007; Jahn et al., 2012; Serreze et al., 2006; Shu et al., 2018) freshwater storage and fluxes are defined relative to a reference salinity, $S_{\text{ref}} = 34.8$. Liquid freshwater storage is defined as the volume of all water with a salinity fresher than S_{ref}, where S is salinity, A is the horizontal area, and h is the depth of the S_{ref} isohaline:

$$V_{fw}(S) = \int_A \int_h \frac{S_{ref} - S}{S_{ref}} dz dA \tag{1}$$

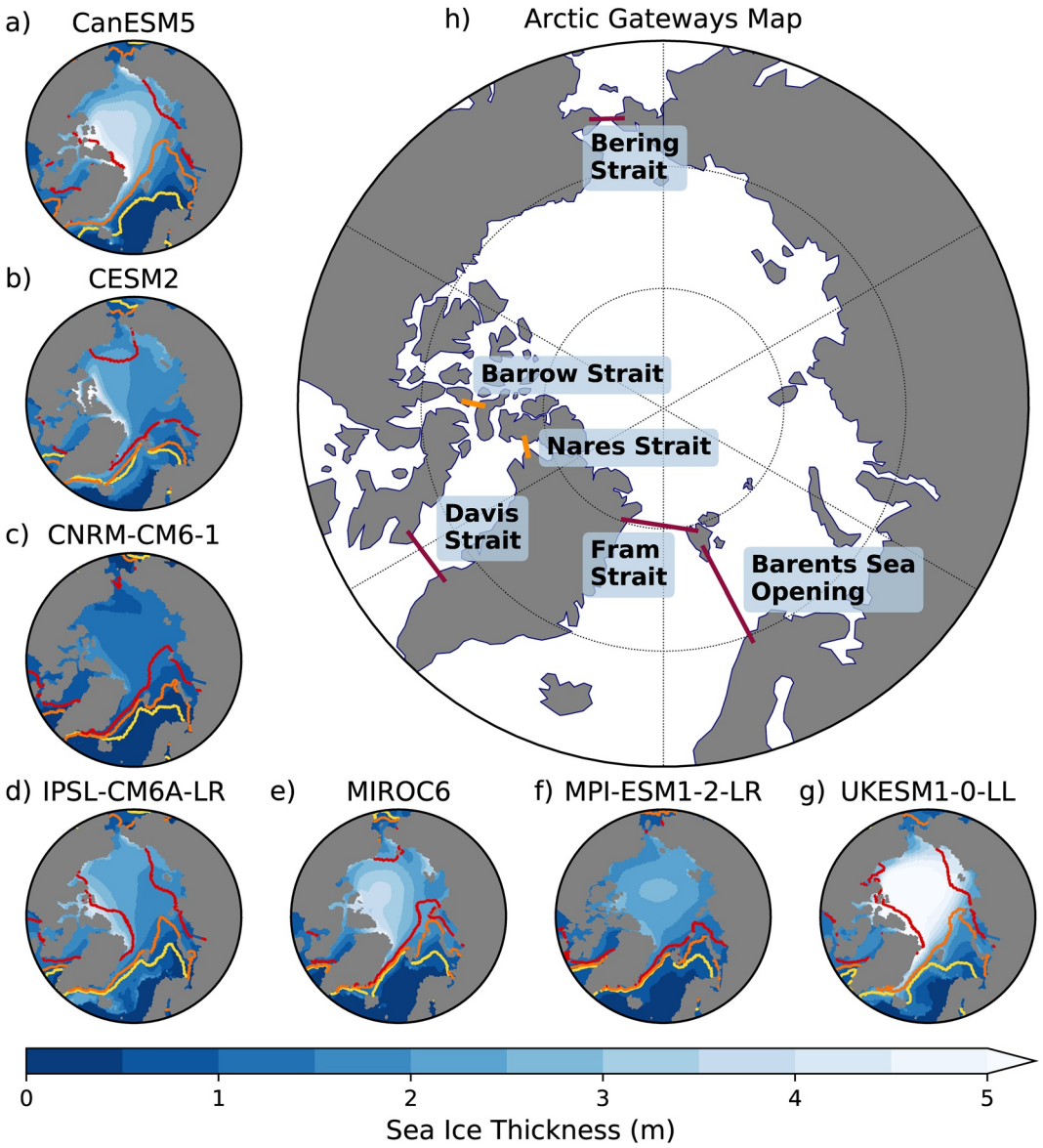

Figure 1. (a–g) Model ensemble mean historical sea ice thickness averaged over 1980–2000 (filled contours) and (h) map of Arctic gateways through which fluxes are computed (dark red and orange lines). Yellow, orange, and red contours in (a–g) denote 15% sea ice concentration for the historical simulation (yellow; 1980–2000 average), SSP1-2.6 (orange; 2080–2100 average), and SSP5-8.5 (red; 2080–2100 average). P-E fluxes, river fluxes, and freshwater storage is computed in the domain bounded by the dark red lines in (h).

Related to the liquid freshwater storage is the liquid freshwater column, defined as the thickness of the water column with salinity fresher than S_{ref}, with h and S defined as in Equation 1:

$$h_{fw}(S) = \int_h \frac{S_{ref} - S}{S_{ref}} dz \tag{2}$$

Liquid freshwater flux is defined as the rate at which freshwater is transported through a face perpendicular to the flow, where $\vec{\mathbf{u}}$ is velocity, S is salinity, L is the length of the strait, and H is the full depth of the water column:

$$F_{fw}(u,S) = \int_H \int_L \frac{S_{ref} - S}{S_{ref}} \vec{\mathbf{u}} \cdot \hat{n} dL dz \quad (3)$$

The sign convention is such that positive $F_{\mathrm{fw}}(u, S)$ is a freshwater flux into the Arctic. Solid storage and fluxes are computed in the same fashion, except that Equations 1 and 3 are multiplied by a solid-to-liquid conversion factor of $\frac{\rho_{ice}}{\rho_{fw}}$ or $\frac{\rho_{snow}}{\rho_{fw}}$ where ρ_{ice}, ρ_{snow}, and ρ_{fw} are the densities of sea ice, snow, and pure freshwater, respectively, and h is the thickness of the sea ice or the snow on top of it.

Schauer and Losch (2019) have argued that salt and volume fluxes should be used instead of ocean freshwater fluxes relative to a reference salinity. Although there are valid reasons for choosing their approach, in particular the ability to understand what is driving variability in freshwater fluxes, we have chosen to use the former approach in order to directly compare the models with observations and previous modeling studies that use the same method to compute the freshwater storage and fluxes (e.g., Haine et al., 2015; Holland et al., 2006, 2007; Serreze et al., 2006). In order to understand the relative importance of velocity versus salinity changes in driving the behavior of the liquid freshwater fluxes, they are also decomposed. The impact of time-varying velocity (u') and time-varying salinity (S') on the freshwater flux is quantified using Equation 3, where $F_{fw}(u', \overline{S})$ is the contribution from the volume flux (associated with transport/velocity change), $F_{fw}(\overline{u}, S')$ is the contribution from the salinity flux, and $\overline{u}$, $\overline{S}$ are the 2000–2100 mean of the given variable in each grid cell. Volume fluxes are also directly computed from the model velocities and are defined as in Equation 3 but with the expression for salinity removed.

2.2. CMIP6 Simulations and Models

Three CMIP6 experiments are analyzed here: the CMIP historical simulation (Eyring et al., 2016), and two future emissions scenarios from ScenarioMIP, SSP1-2.6 and SSP5-8.5 (Shared Socioeconomic Pathways; O'Neill et al., 2016). The historical simulation begins in 1850, ends at the end of 2014, and is forced with observations of emissions and concentrations of greenhouse gases, land use, solar radiation, and stratospheric aerosols, among others. The SSPs begin in 2015 and end in 2100. Of the four SSPs that are updates to the CMIP5 RCPs (Representative Concentration Pathways; Taylor et al., 2012), the two chosen here span the range of simulated radiative forcing at the end of the 21st century, allowing us to assess the range of possible future Arctic freshwater storage and fluxes. With a 2.6 W m^{-2} radiative forcing anomaly at the end of the 21st century, SSP1-2.6 is the lowest warming projection, while SSP5-8.5 is the highest warming projection, with an 8.5 W m^{-2} radiative forcing anomaly at the end of the 21st century.

The following variables are used to calculate the solid and liquid Arctic freshwater storage and fluxes: sea ice thickness (sithick), sea ice snow thickness (sisnthick), sea ice concentration (siconc), sea ice zonal and meridional velocity (siu and siv, respectively), ocean salinity (so), and ocean zonal and meridional velocity (u and v, respectively). River fluxes (friver or vsfriver) and atmospheric precipitation (pr) minus evaporation (evspsbl) fluxes (hereafter, P-E) into the Arctic Ocean are also computed. To quantify the impact of internal variability on model differences and for robust comparisons with observations, only models with at least 10 ensemble members available for the historical simulation are used, although fewer ensemble members are typically available for the SSPs. Although 10 ensemble members is on the lower end of what should be considered a robust sample size from a statistical perspective, this minimum sample size threshold ensures that any errors made as a result of assuming a normal distribution for each model remain small. A total of seven CMIP6 models met these criteria by May 2020 (the last date we checked for new models or model updates): CanESM5, CESM2, CNRM-CM6-1, IPSL-CM6A-LR, MIROC6, MPI-ESM1-2-LR, and UKESM1-0-LL. All model versions used here are nominally 1° in their ice and ocean components, although for virtually all of them the latitude and/or longitude grid spacing is several tenths of a degree above or below this value. Ensemble members are the r*i1p1f1 variant except for CanESM5 (r*i1p2f1), CNRM-CM6-1 (r*i1p1f2), and UKESM1-0-LL (r*i1p1f2). The number of ensemble members used for each experiment, the datasets used, and other information, such as sea ice and snow densities for each model are summarized in Table 1. Model sea ice density, snow density, and sea ice salinity were compiled from ES-DOC (https://es-doc.org/cmip6/). If these values were unavailable, if no time-varying field was found in the model output on the Earth Sys-

Table 1
Summary of the Models Used in This Study, Their Ice and Ocean Components, the Data Sets Used, the Number of Ensemble Members Used From Each Experiment (Historical, SSP1-2.6, and SSP5-8.5), the Sea Ice Density, Snow Density, and Sea Ice Salinity Used to Compute the Solid and Liquid Freshwater Storage and Fluxes, and the Total Volume of the Arctic Domain. The Density of Pure Freshwater (ρfw) Used for all Calculations is 1,000 kg m−3.

Model	Sea ice/ocean components	Historical	SSP1-2.6	SSP5-8.5	ρ_{ice} (kg m^{-3})	ρ_{snow} (kg m^{-3})	S_{ice}	Arctic volume ($\times 10^6$ km^3)	Data sets
CanESM5	LIM2/canNEMO (NEMO3.4.1)	10	10	10	900	330	6	13.8	Swart et al. (2019a, 2019b, 2019c)
CESM2	CICE5.1.2/POP2	11	3	3	917	330	4	13.5	Danabasoglu (2019a, 2019b, 2019c)
CNRM-CM6-1	Gelato6.1/NEMO3.6	19	6	5	917[a]	330[a]	4[a]	13.6	Voldoire (2018, 2019a, 2019b)
IPSL-CM6A-LR	LIM3/NEMO3.2	32	6	6	917[a]	330[a]	4[a]	13.5	Boucher et al. (2018, 2019a, 2019b)
MIROC6	COCO4.9	10	3	3	900	330	5	14.4	Tatebe and Watanabe (2018, 2019a, 2019b)
MPI-ESM1-2-LR	MPI sea ice model/ MPIOM1.6.3	10	10	10	910	330	5	14.5	Wieners et al. (2019a, 2019b, 2019c)
UKESM1-0-LL	GSI8 (CICE5.1.2)/GO6 (NEMO)	13	5	5	917	330	4	13.8	Tang et al. (2019a, 2019b, 2019c)

[a]Denotes an assumed value used for computing the freshwater storage and fluxes because the true value was unavailable. Refer to Section 2.2 for further details.

tem Grid (https://esgf-node.llnl.gov/projects/cmip6/), or if it was unclear from the model documentation whether or not the time-varying field (such as sea ice salinity) was only internal to the particular model component (and thus did not impact freshwater), a sea ice salinity of 4, a sea ice density of 917 kg m^{-3}, and a snow density of 330 kg m^{-3} were used, which are the values from CESM2. For all calculations, the density of pure freshwater (ρ_{fw}) is 1000 kg m^{-3}.

Although the historical simulation begins in 1850, only 1980 onward is considered for our analysis, as it overlaps with observational freshwater budget compilations (Haine et al., 2015; Serreze et al., 2006). Monthly output is used to compute the freshwater storage and fluxes, but for visual clarity annual means are presented in all time series. For all other plots, 20-year means at the end of the 20th and 21st centuries are used—1980–2000 for the historical simulation and 2080–2100 for SSP1-2.6 and SSP5-8.5. Ensemble means are defined as the mean of the ensemble members for each model. The multimodel mean is the mean of the seven model ensemble means, not the mean of all the ensemble members across the models weighted equally, as this would weight models with more ensemble members more strongly. Because our main focus is on storage and flux changes, and not on a full budget analysis or the dynamical reasons behind the simulated changes, we only provide multimodel mean values of P-E and river fluxes across the experiments. Furthermore, no river flux output is available for MPI-ESM1-2-LR, so it is excluded from the multimodel mean, and only one ensemble member is available for MIROC6 for each experiment.

2.3. Historical Simulation Comparison to Observations

Years 1980–2000 from the historical CMIP6 model simulations are compared to 1980–2000 flux observations from Haine et al. (2015) and Prinsenberg and Hamilton (2005), and salinities from the Polar Hydrographic Climatology 3.0 (PHC3.0, updated from Steele et al., 2001) are used to compute the observed freshwater column. No reliable, longer term observations for both solid and liquid fluxes exist for Nares Strait prior to 2000, so in this strait the historical simulation is compared to 2003–2009 values from Münchow (2016). Comparing model 1980–2000 Nares Strait fluxes to the 2003–2009 observations rather than model fluxes over 2000–2010 makes no difference to the results.

Model performance is determined by a graduated scale that bins models based on an observational error multiplier, n, that denotes the number of observed error widths away from the observed value that each model falls. Models with at least one ensemble member that falls within ±1× the observed error have $n = 1$ and are considered comparable to observations. Models with at least one ensemble member that falls within ±2× the observed error have $n = 2$, and so on. The larger the value of n, the poorer the model performs compared to observations. Due to the single ensemble member threshold, only the first 10 ensemble

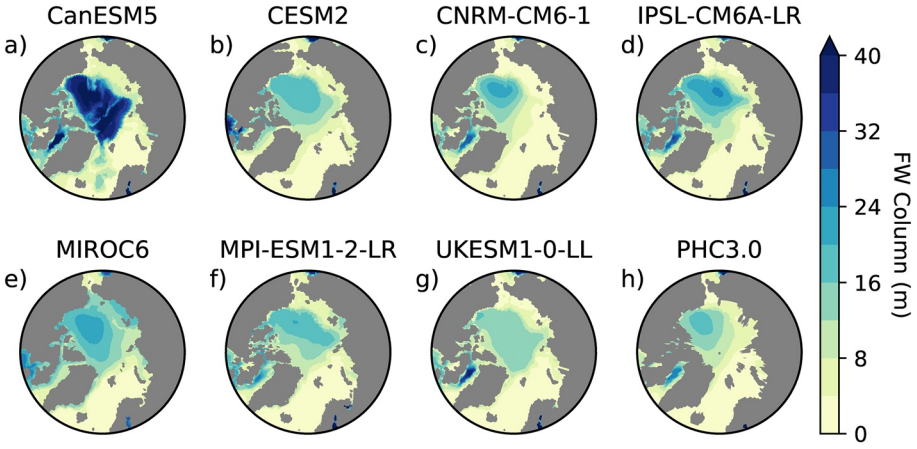

Figure 2. (a–g) Model ensemble mean historical freshwater column (m) averaged over 1980–2000, and (h) freshwater column computed from observed salinities from the Polar Hydrographic Climatology 3.0 (PHC3.0, updated from Steele et al. [2001]).

members from each simulation are used so as not to provide an unfair advantage to models with more ensemble members, although the results are largely insensitive to this choice. For the Barrow Strait solid and liquid fluxes, the Barents Sea Opening and Davis Strait solid fluxes, and the solid and liquid storage, no observational error is available in Haine et al. (2015) and Prinsenberg and Hamilton (2005). In these cases, the mean of all existing observed errors as a percentage of their respective observed values is used in lieu of an observational error. This mean error percentage is 27.5%, and thus for each observation without an error, 27.5% of the observed value is used as the error. The overall conclusions are insensitive to the choice of error, but different error choices do slightly change the n metric in some cases.

3. Results

3.1. Historical Freshwater Storage and Fluxes

Large model differences exist in both the solid and liquid freshwater storage over the historical (1980–2000) period. These differences are apparent in the spatial pattern of the freshwater storage, which is directly related to sea ice thickness (Figure 1) and the freshwater column (Figure 2), and in the pan-Arctic averages (Figure 3).

Sea ice thicknesses in CanESM5, MIROC6, and UKESM1-0-LL are higher over more of the Arctic basin compared to the four remaining models (Figure 1). Of the seven models analyzed, CNRM-CM6-1 has the thinnest ice in the Arctic basin and UKESM1-0-LL the thickest. The areal sea ice coverage also differs across the models, especially in the Barents Sea (Figure 1; yellow line showing the historical 15% sea ice concentration contour). IPSL-CM6A-LR, MIROC6, and MPI-ESM1-2-LR have the lowest sea ice concentrations in this region toward Novaya Zemlya and the inner Barents Sea. As a result of the differences in sea ice thickness and areal coverage, historical ensemble mean solid freshwater storage values vary by a factor of 3, ranging from $\sim 0.91 \times 10^4$ km^3 in CNRM-CM6-1 to $\sim 3.0 \times 10^4$ km^3 in UKESM1-0-LL (Figure 3a). CanESM5 and MIROC6 also exhibit high ensemble mean solid freshwater storage, consistent with their higher Arctic basin sea ice thicknesses (Figures 1a and 1e) as compared to most of the other models. These two models are also closest to the 1980–2000 observed value (Figure 3a; vertical dashed line). The multimodel mean solid freshwater storage is 1.6×10^4 km^3, which is smaller than observations (Table 2).

The historical liquid freshwater storage also varies greatly between models, reflecting large differences in simulated Arctic salinities. The general spatial pattern is similar between most models and PHC3.0, with a maximum in the Beaufort Sea region (Figure 2), but large variations in model salinity are apparent in Baffin Bay, where CanESM5, CNRM-CM6-1, IPSL-CM6A-LR, and UKESM1-0-LL show freshwater columns of >25 m. These Baffin Bay values are larger than those from PHC3.0, which are ~20 m. Integrated over the Arctic, intermodel salinity differences lead to variations of more than a factor of 2 in the simulated liquid

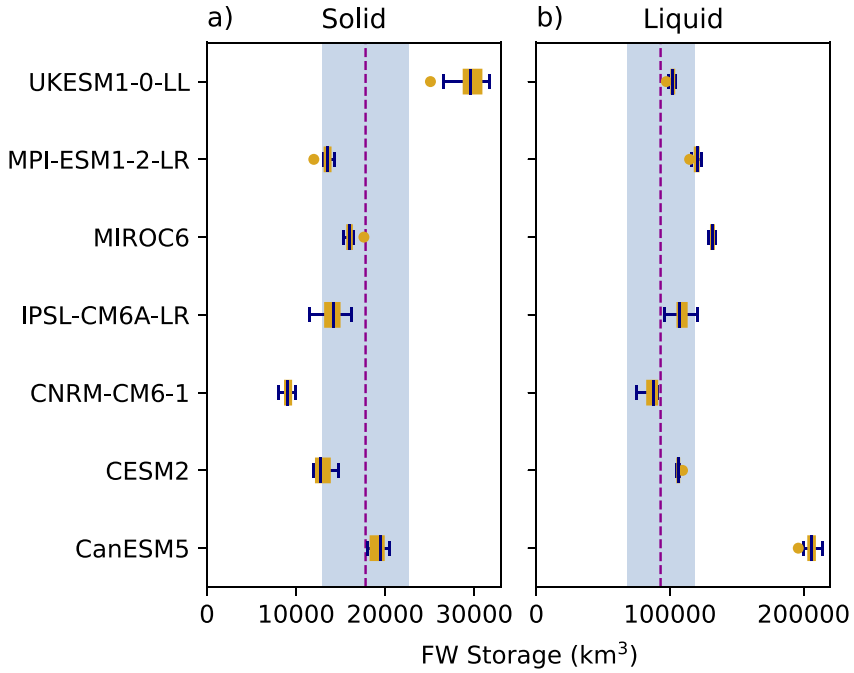

Figure 3. Box-and-whisker plots of (a) solid and (b) liquid freshwater storage (km^3) during the historical period (1980–2000 average) for each model's ensemble members. Boxes delineate the interquartile range (IQR), the navy line inside each is the median, whiskers extend to 1.5× the IQR, and fliers (outliers) appear as dots. Vertical dashed lines are observed values over 1980–2000 from Haine et al. (2015). Blue shading denotes an estimated error that is 27.5% of the observed value (refer to Section 2.3 for further details) as no observed error is provided in Haine et al. (2015).

freshwater storage over the historical period (Figure 3b). The starkest contrast in the freshwater content is found between CanESM5 and the remaining six models (Figure 2). Maximum values of the freshwater column in CanESM5 are >35 m over much of the Arctic basin, while for the other models maximum values are ~10 m lower (Figure 2). As a result, CanESM5 has the largest liquid freshwater storage by far (Figure 3b), with $\sim 2.1 \times 10^5$ km^3, while CNRM-CM6-1 has the smallest with $\sim 0.86 \times 10^5$ km^3. The ensemble mean liquid freshwater storage values from CNRM-CM6-1 and UKESM1-0-LL are closest to observations (Figure 3b; vertical dashed line), and occur on the low end of the model spread. The multimodel mean liquid freshwater storage is 1.2×10^5 km^3 (Table 2), which is higher than observations, mostly due to the very high freshwater storage in CanESM5.

The ensemble member spreads for each model are also different, and differences between the ensemble members of each model (intramodel spread) are typically smaller than the differences between models (intermodel spread) for both solid and liquid freshwater storage. This indicates that, at least for this subset of CMIP6 models, intermodel differences in freshwater storage are due more to model biases rather than internal variability. However, a portion of the differences in intramodel spreads is related to the number of ensemble members for each model (Table 1). Model Arctic Ocean volumes also vary, ranging between 13.5 and 14.5×10^6 km^3 (Table 1). This difference contributes to the liquid freshwater storage differences between models, but it does not account for all of them, as it does not explain a difference of more than a factor of 2. A liquid freshwater storage of 10^5 km^3 for an Arctic Ocean volume of 13.5×10^6 km^3 is equivalent to a freshwater storage of $\sim 1.07 \times 10^5$ km^3, or a 7% freshwater increase, for an Arctic Ocean with a volume of 14.5×10^6 km^3. For a freshwater storage of 2×10^5 km^3—much larger than that of most of the models used here—the percentage difference in freshwater storage due to volume variation doubles to 14%.

Similar to the solid and liquid freshwater storage, historical solid and liquid freshwater fluxes through the Arctic gateways also vary considerably between models (Figure 4), with very few consistently close to observations. For the solid fluxes (Figures 4a–4f) fewer than four models (typically 1–2) are close to observations for any given location. Little pattern or consistency exists between models over- or underestimating the solid fluxes in any of the straits except for Davis Strait and the Barents Sea Opening, where all or most of

Table 2
Multimodel Mean, Time Mean P–E (Precipitation Minus Evaporation) Fluxes, River Runoff, and Solid and Liquid Freshwater Storage and Fluxes Averaged Over the Historical Simulation (1980–2000) and SSP1–2.6 and SSP5–8.5 (2080–2100). Observations over 1980–2000 are noted parenthetically and are from Haine et al. (2015), Munchow (2016) (Nares Strait only, refer to Section 2.3 for further details), Prinsenberg and Hamilton (2005), and Serreze et al. (2006).

	Historical	SSP1-2.6	SSP5-8.5
External fluxes (km^3 $year^{-1}$)			
River runoff[a]	3546 (3900 ± 390)	4084	5605
P-E	2100 (2000 ± 200)	2211	2494
Storage (km^3)			
Solid	16431 (17800)	5561	1275
Liquid	122733 (93000)	166768	195880
Solid fluxes (km^3 $year^{-1}$)			
Bering Strait	77 (140 ± 40)	16	−1
Nares Strait	−125 (−252 ± 63)	−56	−21
Barrow Strait	−30 (−76)	−17	−5
Fram Strait	−1739 (−2300 ± 340)	−625	−96
Barents Sea Opening	−184 (−40)	−14	0
Davis Strait	−515 (−160)	−310	−93
Liquid fluxes (km^3 $year^{-1}$)			
Bering Strait	2203 (2400 ± 300)	2203	2362
Nares Strait	−1231 (−1356 ± 236)	−1626	−2010
Barrow Strait	−484 (−1510)	−318	−696
Fram Strait	−2111 (−2700 ± 530)	−4566	−5595
Barents Sea Opening	−350 (−90 ± 90)	708	1605
Davis Strait	−2542 (−3200 ± 320)	−2819	−4230

[a]The multimodel mean river fluxes exclude MPI-ESM1-2-LR and only include one ensemble member for MIROC6.

the models overestimate the flux magnitude. For some of the smallest solid freshwater fluxes, in the Bering (Figure 4a), Nares (Figure 4b), and Barrow (Figure 4c) straits, a few models disagree on the sign of the solid fluxes, likely reflecting noise in an area where there is little sea ice flux. The spread in solid flux within the members of each model is often smaller than the differences between models, although the Barents Sea solid flux, albeit small, is a counterexample (Figure 4e). For the liquid freshwater fluxes (Figures 4g–4l), the models are closer to observations. Models both over- and underestimate the liquid fluxes in any given strait except in Barrow Strait, where they all underestimate the magnitude of the flux. The only sign disagreement between models occurs for the liquid flux through the Barents Sea Opening (Figure 4k), where some ensemble members for CanESM5 and IPSL-CM6A-LR show a positive freshwater flux. Overall, there is closer intermodel agreement for the liquid fluxes than the solid fluxes, as shown by more overlap between the models' ensemble member spreads (Figure 4). For this subset of CMIP6 models, the multimodel mean fluxes are also either overestimated or underestimated relative to observations (Table 2), except for the liquid fluxes in the Bering and Nares straits.

A summary of model performance compared to observations (Figure 5) indicates that based on our metric (Section 2.3) the models are better at simulating freshwater storage than they are at simulating freshwater fluxes. For both the solid and liquid storage (Figure 5c), five of the seven models agree well with observations, although it is not the same five models for each component. The models are poorer at simulating the historical solid fluxes compared to the liquid fluxes, with three models or fewer agreeing with observations in any given strait for the former (Figure 5a). For the Davis Strait solid flux, only two models fall within 5× the observational error range. The liquid flux performance (Figure 5b) is better, with more models exhibiting a smaller error multiplier (Figure 5b; darker greens) in more of the straits, and only two instances of models falling outside 5× the observational error range. The Fram Strait liquid fluxes fall within 3× the observational error range for all models, and within 2× the observational error range for six models. Overall, IPSL-CM6A-LR exhibits the best agreement with observations across the largest number of straits for the liquid fluxes and for solid and liquid storage.

3.2. Future Freshwater Storage and Fluxes in SSP1-2.6 and SSP5-8.5

In both future emissions scenarios model freshwater storage at the end of the 21st century (2080–2100) is characterized by drastic declines in solid storage and increases in liquid freshwater storage (Figure 6, Table 2). In all models, the reduction in solid storage is much larger for SSP5-8.5 than for SSP1-2.6 (Figure 6a) due to larger sea ice decline in the stronger forcing scenario (Figure 1; orange and red lines). The ice loss simulated under SSP5-8.5 is so large in some models that the central Arctic is ice-free in the annual mean by the end of the 21st century, with remaining sea ice confined to the margins of Eurasia and North America (e.g., CanESM5, IPSL-CM6A-LR, and UKESM1-0-LL; Figure 1, red lines; Figure S1). Liquid freshwater storage (Figure 6b) increases are larger for SSP5-8.5 than SSP1-2.6 in all models except IPSL-CM6A-LR, where the liquid freshwater storage change is the same under both scenarios, despite differences in the simulated solid freshwater storage. Ice melt as well as increases in river and P-E fluxes (Table 2) drive most of the multimodel mean increase in liquid storage in both future scenarios. Although trends in the multimodel mean solid and liquid storage are apparent in the historical simulation, SSP-driven differences in future storage do not become apparent until ~2040 for solid storage and ~2050 for liquid storage (Figures 6c and 6d). By the end of the 21st century, model max/min envelopes for the two scenarios no longer overlap for solid storage while for liquid storage the multimodel mean for SSP5-8.5 is still within the envelope of SSP1-2.6. This is

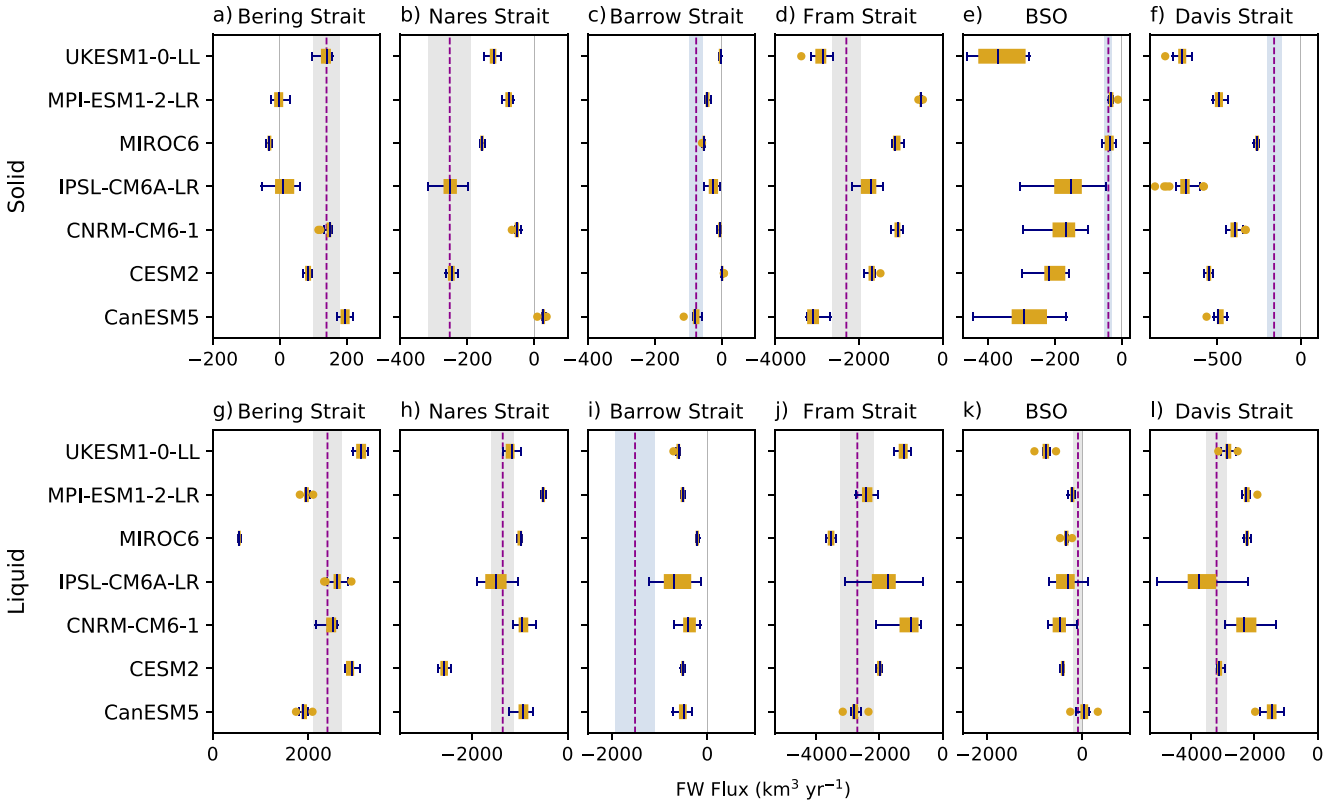

Figure 4. Ensemble spreads of (a–f) solid and (g–l) liquid freshwater fluxes (km^3 yr^{-1}) through (a, g) Bering Strait, (b, h) Nares Strait, (c, i) Barrow Strait, (d, j) Fram Strait, (e, k) the Barents Sea Opening, and (f, l) Davis Strait during the historical period (1980–2000 average) for each model. Vertical dashed lines denote observed values over the same period (except for Nares Strait) and gray shading the error from Haine et al. (2015) and Prinsenberg and Hamilton (2005). Nares Strait observations are from Münchow (2016) and cover 2003–2009. In locations where no observed error is provided in Haine et al. (2015) or Prinsenberg and Hamilton (2005), blue shading denotes an estimated error that is 27.5% of the observed value (refer to Section 2.3 for further details).

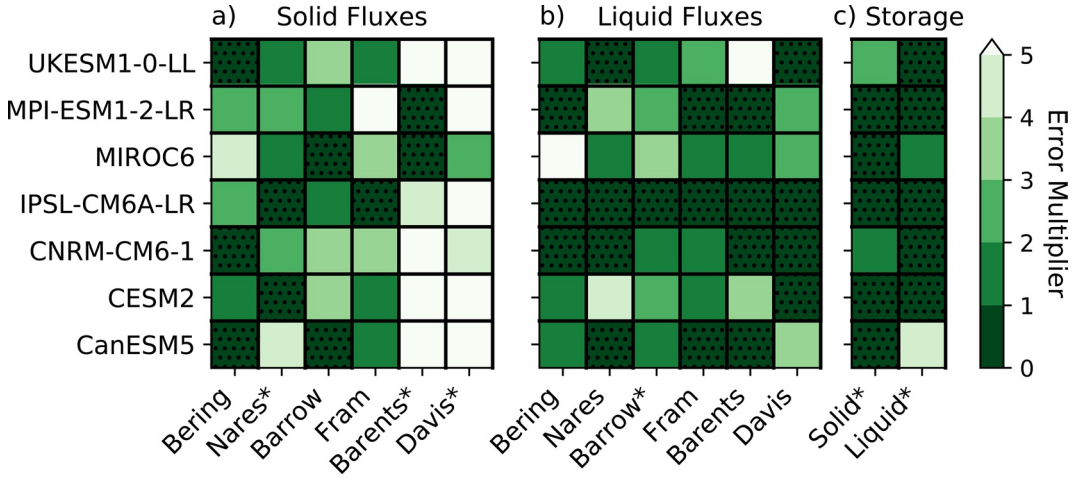

Figure 5. Summary of model performance over the historical period (1980–2000 average) compared to observations for (a) solid fluxes, (b) liquid fluxes, and (c) storage. Models are binned based on their proximity to the observational error range, i.e., an error multiplier of 1 indicates that the model falls within the observational error bounds for at least one ensemble member, an error multiplier of 2 indicates that the model falls within 2 times the observational error bounds for at least one ensemble member, etc. Stippling further indicates that a model is within the observational error for a given location. For locations without an observational error estimate (*x*-axis names marked by an asterisk), an error of 27.5% of the observed value is used. Refer to Section 2.3 for further details.

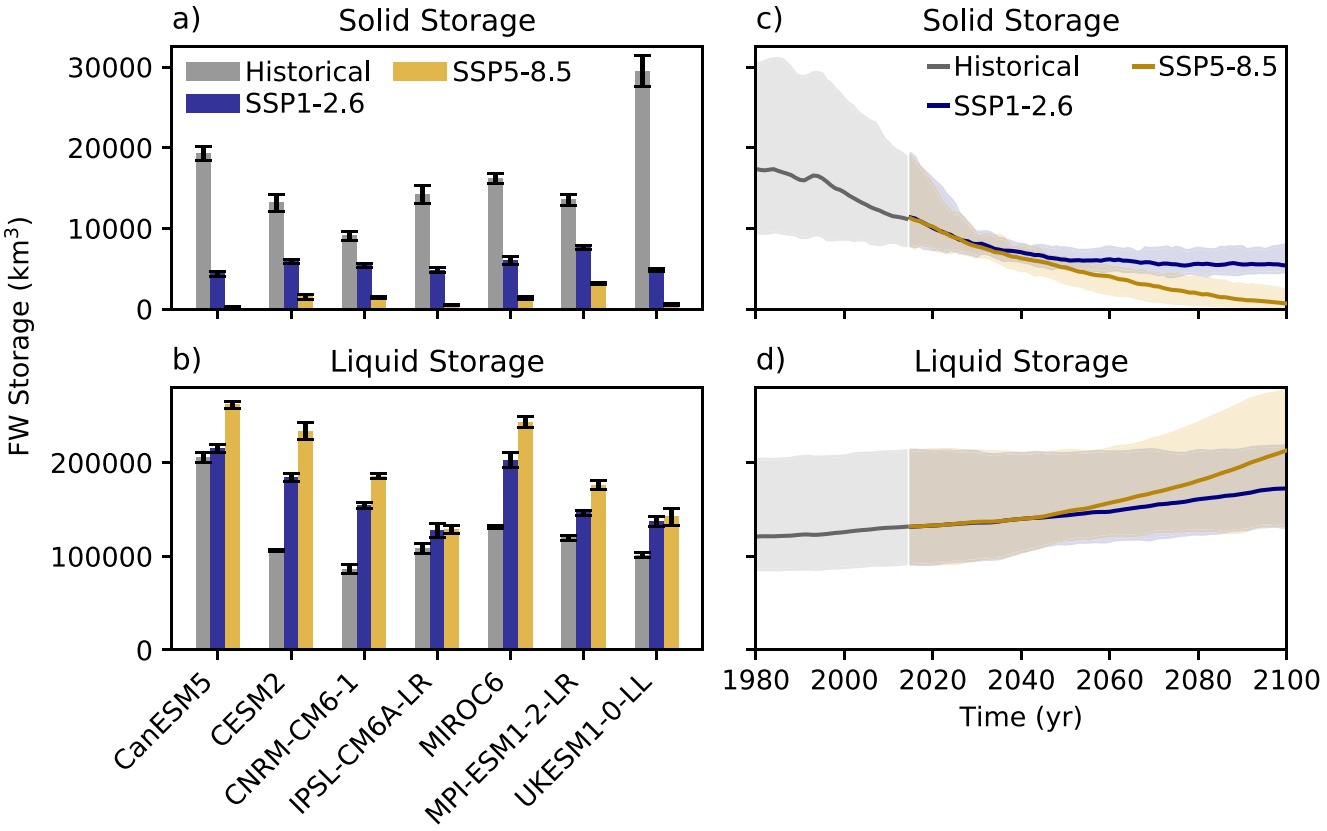

Figure 6. Model ensemble mean (a) solid and (b) liquid freshwater storage (km^3) for the historical (1980–2000 average), SSP1-2.6 (2080–2100 average), and SSP5-8.5 (2080–2100 average) experiments and multimodel mean (the mean of the models' ensemble means) (c) solid and (d) liquid freshwater storage (km^3) from 1980–2100 for SSP1-2.6 and SSP5-8.5. Error bars in (a) and (b) are ±1 standard deviation of each model's ensemble members. Shading in (c) and (d) spans the maximum and minimum value that any model ensemble mean reaches at a particular time.

primarily due to CanESM5, which has a much larger liquid freshwater storage compared to all other models and so leads to very wide model max/min envelopes in both scenarios.

Concomitant with the decline in solid freshwater storage, solid freshwater fluxes through the Arctic gateways decline as well (Figures 7 and 8, Table 2). In all models solid freshwater flux declines are larger for SSP5-8.5 than for SSP1-2.6 in the Nares (Figure 7b), Fram (Figure 7d), and Davis straits (Figure 7f). In the Bering Strait (Figure 7a), Barrow Strait (Figure 7c), and the Barents Sea Opening (Figure 7e), solid fluxes in most models drop to nearly zero in both scenarios due to a sharp decrease or total disappearance of sea ice in these locations (Figures 1 and S1). In CanESM5 and UKESM1-0-LL, even the Fram Strait solid flux reaches near-zero levels by the end of the 21st century in SSP5-8.5 (Figure 7d), but other models retain a small solid flux there. Multimodel mean differences between the two scenarios for the Nares, Fram, and Davis solid fluxes are distinguishable beginning in ~2050–2060 (Figures 8b, 8d, and 8e), but are largest at the end of the 21st century, where for Fram (Figure 8d) and Davis (Figure 8f) straits the max/min envelopes for the scenarios no longer overlap. Scenario differences in the remaining straits (Figures 8a, 8c, and 8e) are largely indistinguishable over the 21st century.

Liquid freshwater fluxes (Figures 9 and 10, Table 2) generally increase in magnitude over the 21st century in both SSP1-2.6 and SSP5-8.5. However, the magnitude of the liquid flux changes varies widely across models, and sometimes the multimodel mean reflects a cancellation of these large disparities rather than a robust behavior that is present in each model. Models agree best for the projected changes in Fram Strait and the Barents Sea Opening and differ the most in Bering Strait and the straits west of Greenland.

All models show an increase in the Fram Strait liquid freshwater flux that is stronger in SSP5-8.5 than SSP1-2.6 at the end of the 21st century, except in CESM2, where it is stronger in SSP1-2.6 (Figure 9d). The

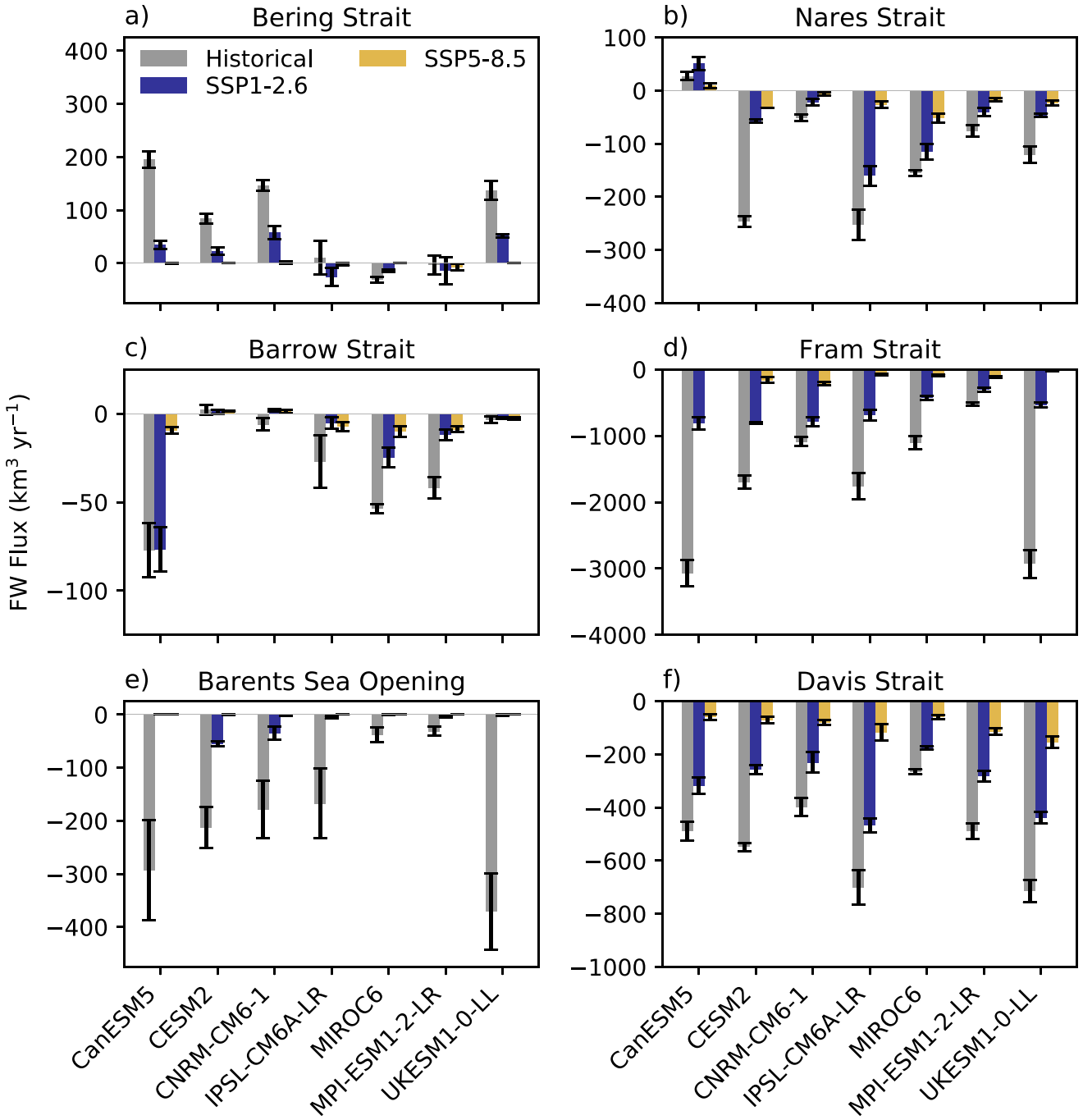

Figure 7. Model ensemble mean solid freshwater flux (km^3 yr^{-1}) at (a) Bering Strait, (b) Nares Strait, (c) Barrow Strait, (d) Fram Strait, (e) the Barents Sea Opening, and (f) Davis Strait for the historical (1980–2000 average), SSP1-2.6 (2080–2100 average), and SSP5-8.5 (2080–2100 average) experiments. Error bars are ±1 standard deviation of each model's ensemble members.

multimodel mean increase in freshwater export (Figure 10d) is strongest in the first half of the 21st century, after which it levels off, and is driven by an equal combination of freshening and an increase in the volume flux (Figure 11d).

In the Barents Sea Opening, the liquid freshwater fluxes reverse sign under both scenarios in the multimodel mean (Figure 10e and Table 2) and in nearly all models (Figures 9e and S7), except for MPI-ESM1-2-LR where it occurs under SSP5-8.5 only and CanESM5, where the historical liquid flux is indistinguishable

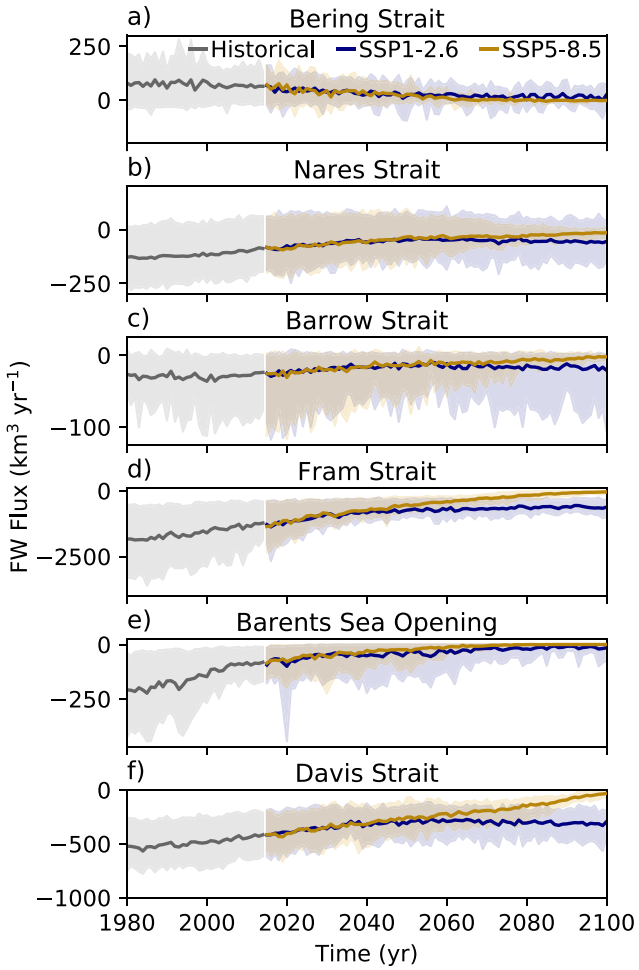

Figure 8. Multimodel mean (the mean of the models' ensemble means) solid freshwater flux (km^3 yr^{-1}) from 1980–2100 at (a) Bering Strait, (b) Nares Strait, (c) Barrow Strait, (d) Fram Strait, (e) the Barents Sea Opening, and (f) Davis Strait for SSP1-2.6 and SSP5-8.5. Shading spans the maximum and minimum value that any model ensemble mean reaches at a particular time.

from zero. The sign reversal is due to a strong freshening that occurs throughout the 21st century, which is indicated by the positive trend in the salinity flux anomaly contribution (Figure 11e). The volume flux anomaly contribution remains fairly constant and small in comparison, and the absolute volume fluxes in each model (Figure S7) remain positive and generally increase over this period, further corroborating a salinity-driven sign change.

In the Bering Strait, individual models show either small increases in fluxes (CanESM5, MPI-ESM1-2-LR, and UKESM1-0-LL), small decreases (CESM2 and MIROC6), or no change (CNRM-CM6-1 and IPSL-CM6A-LR), but the multimodel mean liquid flux is fairly stable over 1980–2100 (Figure 10a and Table 2). The stable multimodel mean is due to compensating contributions from the volume and salinity fluxes in both scenarios, with a freshening of the inflow that is counteracted by a decrease in the volume flux (Figure 11a). However, even though all models show the same general physical behavior as the multimodel mean, the magnitude of their volume and salinity anomalies vary, leading to liquid freshwater flux changes with different signs (Figures 9a and S3).

West of Greenland in the Nares (Figure 9b), Barrow (Figure 9c), and Davis (Figure 9f) straits, liquid freshwater export mostly increases in both scenarios (Table 2) and in most models, although there is considerable model disagreement in Barrow Strait (Figure 9c). CNRM-CM6-1 deviates most strongly from this pattern of increasing export, with decreases in Nares and Davis straits and a flux sign reversal in Barrow Strait. In the multimodel mean, the increase in liquid freshwater export does not begin until after mid-century (Figures 10b, 10c, and 10f), due to a decrease in the volume flux that opposes the freshening of the outflowing water (Figures 11b, 11c, and 11f). After mid-century the volume flux increases again, and along with the continued freshening of these waters, leads to an increase in the multimodel mean freshwater exported from these straits. However, similar to the Bering Strait, the multimodel mean liquid freshwater flux change (Figures 10b, 10c, and 10f) is not robust across models and is instead the result of averaging over major intermodel differences (Figures 9b, 9c, 9f, S4, S5, and S8). Despite these differences, all models show the same physical behavior: a decrease in the volume export over the early 21st century and an increase or stabilization thereafter (Figure 12), coupled with continuously decreasing salinity over the entire 21st century (Figures S4, S5, and S8). Although the salinity change is captured by the multimodel mean (Figure 11), the timing and magnitude of the volume export varies strongly between models (Figure 12), and as a result the liquid freshwater export does as well (Figures S4, S5, and S8).

To summarize, the consistent results across models are that by the end of the 21st century in both emissions scenarios the magnitude of the solid fluxes decreases in all straits, solid freshwater storage decreases, and liquid freshwater storage increases (Figure 13, Table 2). The models show poorer agreement on the direction of the liquid flux changes (Figures 13b and 13e), where for example, in the Bering and Davis straits in SSP1-2.6 (Figure 13b), a similar number of models suggest an increase, decrease, or no change relative to the historical period (1980–2000). For SSP5-8.5 (Figure 13e) a larger number of models agree that the magnitude of the liquid fluxes will increase in most of the straits, although in some straits (especially Bering, Barrow, Nares, and Davis) certain models still suggest no change in the fluxes or a decrease in magnitude. In the Barents Sea, six models indicate a change in sign of the flux (Figure 13e) and of these, five exhibit a magnitude increase as well. CanESM5 also exhibits a magnitude increase, but because its historical flux is indistinguishable from zero (Figure 9e), a sign change technically does not occur. All of the models show an increase in the magnitude of the liquid freshwater flux through Fram Strait in both scenarios (Figures 13b

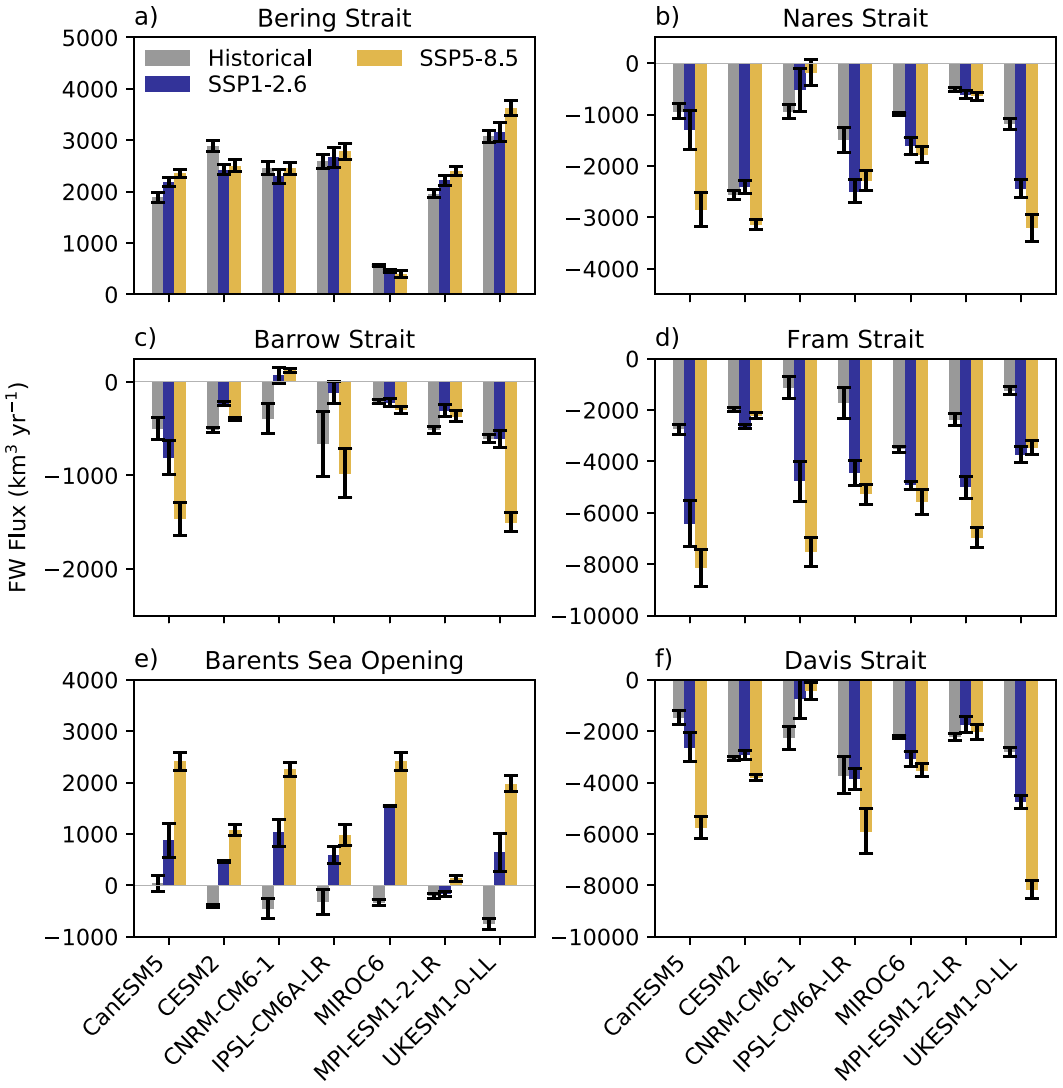

Figure 9. Model ensemble mean liquid freshwater flux (km^3 yr^{-1}) at (a) Bering Strait, (b) Nares Strait, (c) Barrow Strait, (d) Fram Strait, (e) the Barents Sea Opening, and (f) Davis Strait for the historical (1980–2000 average), SSP1-2.6 (2080–2100 average), and SSP5-8.5 (2080–2100 average) experiments. Error bars are ±1 standard deviation of each model's ensemble members.

and 13e), making this the most robust projected liquid flux change. The same is true for the solid fluxes in the Fram and Davis straits and the Barents Sea Opening, where all models project decreases in both scenarios.

4. Discussion

Simulated historical (1980–2000) Arctic freshwater storage and fluxes in seven CMIP6 models show considerable disparities. For the solid and liquid storage (Figure 3), the solid fluxes (Figures 4a–4f), and to a lesser extent the liquid fluxes (Figures 4g–4l), intermodel differences are larger than the ensemble spreads of individual models, indicating that internal variability alone does not account for the differences in this subset of CMIP6 models. The models also do not show consistent agreement with observations over the historical period, with the exception of IPSL-CM6A-LR, which performs best (Figure 5). Most models underestimate the solid freshwater storage (Figure 3a), overestimate the liquid freshwater storage (Figure 3b), and show poorer agreement between the solid fluxes and observations compared to the liquid fluxes (Figures 4 and 5). The same is true in the multimodel mean (Table 2) which underestimates the solid storage; the Bering,

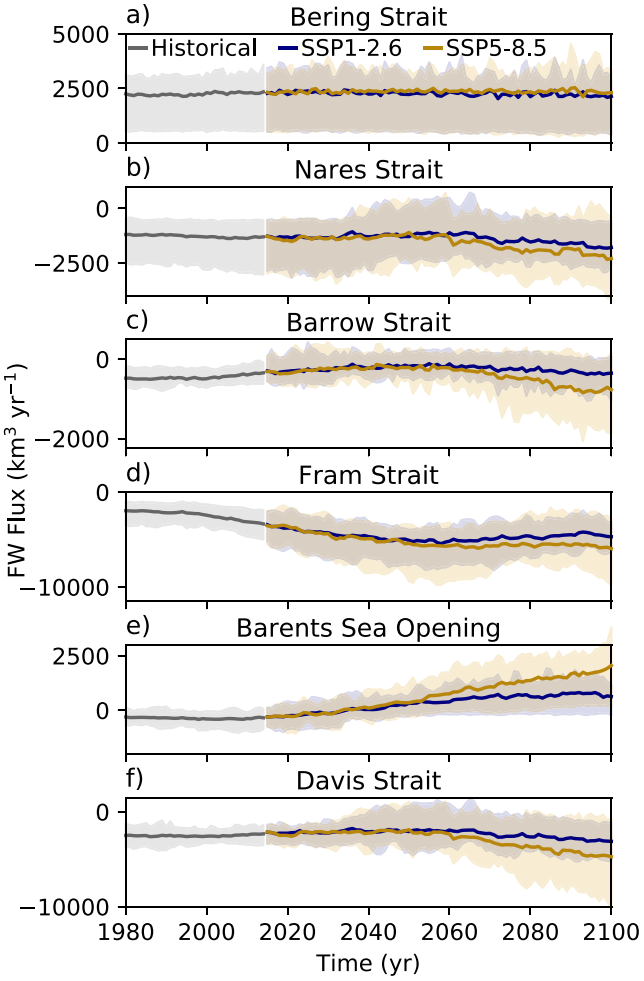

Figure 10. Multimodel mean (the mean of the models' ensemble means) liquid freshwater flux (km^3 yr^{-1}) from 1980–2100 at (a) Bering Strait, (b) Nares Strait, (c) Barrow Strait, (d) Fram Strait, (e) the Barents Sea Opening, and (f) Davis Strait for SSP1-2.6 and SSP5-8.5. Shading spans the maximum and minimum value that any model ensemble mean reaches at a particular time.

Nares, Barrow, and Fram Strait solid fluxes; and the Barrow, Fram, and Davis Strait fluxes, and overestimates the liquid storage; the Barents Sea Opening and Davis Strait solid fluxes; and the Barents Sea Opening liquid flux. Despite the sparsity and incompleteness of observations in the Arctic gateways, observational uncertainty is not responsible for the disagreement between the models and observations, as the models are rarely consistently shifted in one direction for a given strait (and even if they are it could simply indicate that all the models are biased). Instead the simulated fluxes are characterized by large spreads between the models (Figure 4) that no single observational flux—biased or otherwise—could match, effectively precluding the possibility that observational errors can explain the disagreement. The overall lack of agreement with observations suggests that, much like previous model generations (e.g., Holland et al., 2007; Jahn et al., 2012; Shu et al., 2015; Wang et al., 2016a), this newest generation of models still has large mean state biases in sea ice volume and ocean salinity, with generally too little sea ice and too low salinities. However, with only seven models used in this study these multimodel means may not be representative of CMIP6 as a whole, which comprises many more models.

Despite the historical freshwater storage and flux biases, future changes in these quantities (Figures 6–11 and 13, Table 2) show increased liquid freshwater storage and fluxes and decreased solid storage and fluxes over the 21st century, consistent with previous modeling studies (Holland et al., 2006, 2007; Jahn & Laiho, 2020; Koenigk et al., 2007; Shu et al., 2018; Vavrus et al., 2012). As in CMIP3 and CMIP5, the CMIP6 models used in this study also do not have interactive ice sheets and thus do not account for freshwater input from Greenland ice sheet melt (Nowicki et al., 2020). As a result future liquid freshwater storage and flux changes, especially in the straits adjacent to Greenland—Fram Strait, Nares Strait, and Davis Strait—are likely underestimated in all of these simulations and provide a lower bound on the changes we can expect to see. However, all CMIP6 models analyzed here have two gateways west of Greenland, making the simulated fluxes more realistic, whereas only 8 of the 11 CMIP5 models analyzed by Shu et al. (2018) had one or two open gateways.

Combining the solid and liquid freshwater fluxes, we find that the total increase in freshwater export east of Greenland, in the Fram Strait, is larger than the total increase in freshwater export west of Greenland, in the Nares and Barrow straits (or the Davis Strait alone) in both SSP1-2.6 and SSP5-8.5. In the Nares and Barrow straits, decreases in the multimodel mean solid freshwater fluxes (Figures 8b and 8c), which are already small, are eclipsed by increases in the liquid freshwater fluxes (Figures 10b and 10c), resulting in an increase in the total amount of freshwater exported from these locations. The total amount of freshwater exported from the Fram and Davis Straits (Figures 8d, 8f, 10d, and 10f) also increases, even though they are the two largest exporters of sea ice in the late 20th century and exhibit strong declines in sea ice export over the 21st century (Figures 7d, 7f, 8d, and 8f). The strong increases in the Fram and Davis liquid export (Figures 9d, 9f, 10d, and 10f) are consistent with the CMIP5-based results from Shu et al. (2018). In the Barents Sea, solid fluxes are small in magnitude and decline over the 21st century (Figure 8e), while the net liquid freshwater flux shifts from weak export to strong import (Figure 10e) as in previous studies (Holland et al., 2006; Shu et al., 2018).

Models sometimes disagree on the direction of the liquid freshwater flux changes projected over the 21st century (e.g., in Bering Strait and the straits west of Greenland), but they agree much better on the general direction of the salinity and volume flux anomaly changes, but not necessarily on their magnitude (Figures 11 and 12). In Bering Strait, the liquid flux shows little change in its multimodel mean value over the

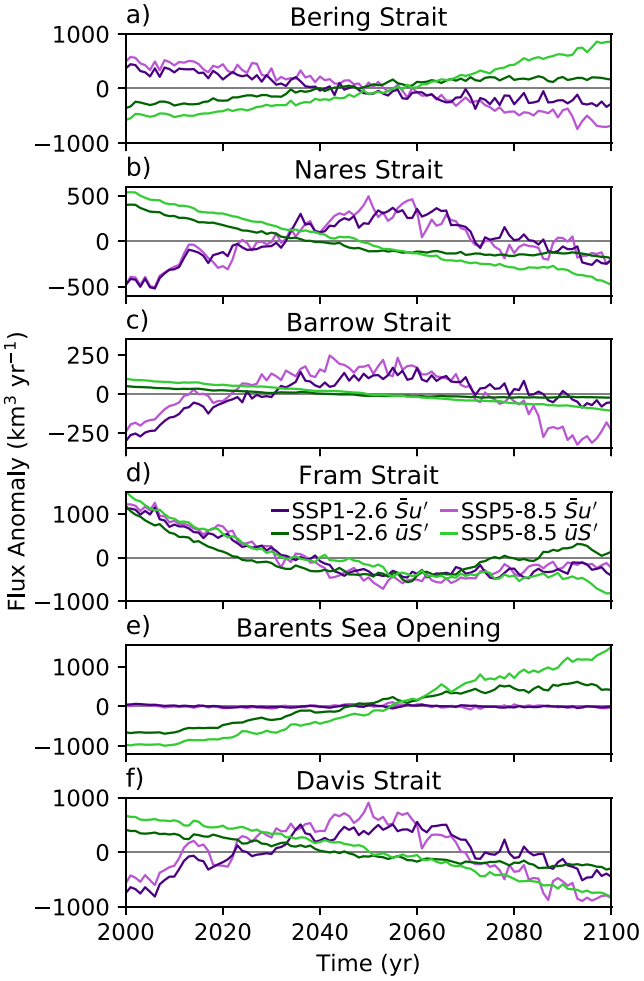

Figure 11. Anomalous contribution of volume ($\bar{S}u'$, purple) and salinity ($\bar{u}S'$, green) fluxes (km^3 yr^{-1}) to the liquid freshwater flux at (a) Bering Strait, (b) Nares Strait, (c) Barrow Strait, (d) Fram Strait, (e) the Barents Sea Opening, and (f) Davis Strait for SSP1-2.6 (darker colors) and SSP5-8.5 (lighter colors). Flux anomalies are computed relative to the 2000–2100 mean in each strait. Due to the difference in sign of the mean fluxes in each strait [positive for (a) and (e) and negative for (b), (c), (d), and (f)] the meaning of a positive or negative trend in the flux contributions changes depending on the strait. For example, a positive trend in the Bering Strait salinity contribution implies a freshening of the Bering Strait waters, while a negative trend in the Nares Strait salinity contribution implies the same for the Nares Strait waters. The strait invariant sign convention is that positive trends imply Arctic Ocean freshening.

21st century (Figure 10a), in contrast to Shu et al. (2018) who show that in CMIP5 the multimodel mean Bering Strait liquid flux increases until the ~2030s and then decreases over the rest of the 21st century in most future forcing scenarios. The CMIP6 multimodel mean Bering Strait liquid flux remains stable throughout the 21st century due to a freshening of the inflowing waters that is compensated by a decrease in their volume flux, as was previously seen in CCSM3, a CMIP3 generation model (Holland et al., 2006). This pattern of anomalies is present in all models (Figure S3), but their relative magnitudes vary, leading to steady, increasing, or decreasing 21st century liquid freshwater fluxes in this location. However, during the very late 20th and early 21st centuries (1990–2015) most models do show a small increase in the freshwater flux, consistent with the CMIP5 models (Shu et al., 2018) as well as observations (Woodgate, 2018), but most also show a decrease or no change in the volume flux over the same period, which has not been observed (Woodgate, 2018).

West of Greenland, in the Nares, Barrow, and Davis straits, freshening is compensated by a decrease in the volume flux during the first half of the 21st century, leading to stable multimodel mean fluxes over this period. Beyond 2050, the multimodel mean freshwater export increases in these straits due to a combination of increasing volume fluxes and continued freshening. Increasing freshwater fluxes west of Greenland during the 21st century have been documented in previous studies (Holland et al., 2006, 2007; Jahn & Holland, 2013; Vavrus et al., 2012). However, these studies do not exhibit the same pattern as the CMIP6 multimodel mean freshwater flux, although some individual models do agree with their findings (Figures S4, S5, S8; IPSL-CM6A-LR, MIROC6, MPI-ESM1-2LR, UKESM1-0-LL), showing an increase in the freshwater export west of Greenland over most of the 21st century that levels off or slightly decreases after the 2070s (Jahn & Holland, 2013; Vavrus et al., 2012). Two models, CESM2 and CNRM-CM6-1, show a strong decline in the freshwater flux, which leads to the steady multimodel mean for the first half of the 21st century. The volume flux in the late 20th and early 21st century decreases in all models, but the magnitude and timing varies (Figure 12), starting between the 1980s and the late 2010s (depending on the model) and peaking between the 2020s and the 2060s before reversing or leveling off. Furthermore, the magnitude of the decrease varies significantly between models, with some even exhibiting a change in the direction of the volume flux through the Barrow, Nares, and/or Davis straits (e.g., IPSL-CM6A-LR and CNRM-CM6-1; Figure 12). However, in all models the volume flux reduces by more than 50%. The overall disagreement between the models in these straits indicates a larger projection uncertainty associated with the fluxes west of Greenland than found for any of the other Arctic gateways.

Even though such an early decline in the volume fluxes west of Greenland has not been reported previously, studies show that the late 21st century volume flux decline west of Greenland is driven by a reduction in the sea surface height gradient between the Labrador Sea and the Arctic Ocean (Houssais & Herbaut, 2011; Jahn & Holland, 2013; Jahn et al., 2010) via an increase in the Labrador Sea sea surface height. In turn, the Labrador Sea sea surface height is correlated with long-term AMOC variations (Saenko et al., 2017). Interestingly, a recent study of AMOC in CMIP6 models has found that many show a peak in AMOC in the 1980s, followed by a decline since then and over the 21st century, in contrast to CMIP5 models that showed a weak decline over the 20th century that accelerated in the 21st century (Weijer et al., 2020). Understanding what drives the volume flux reduction west of Greenland in the CMIP6 models, and whether or not the differences in both the AMOC and the volume flux anomalies between CMIP5 and CMIP6 are

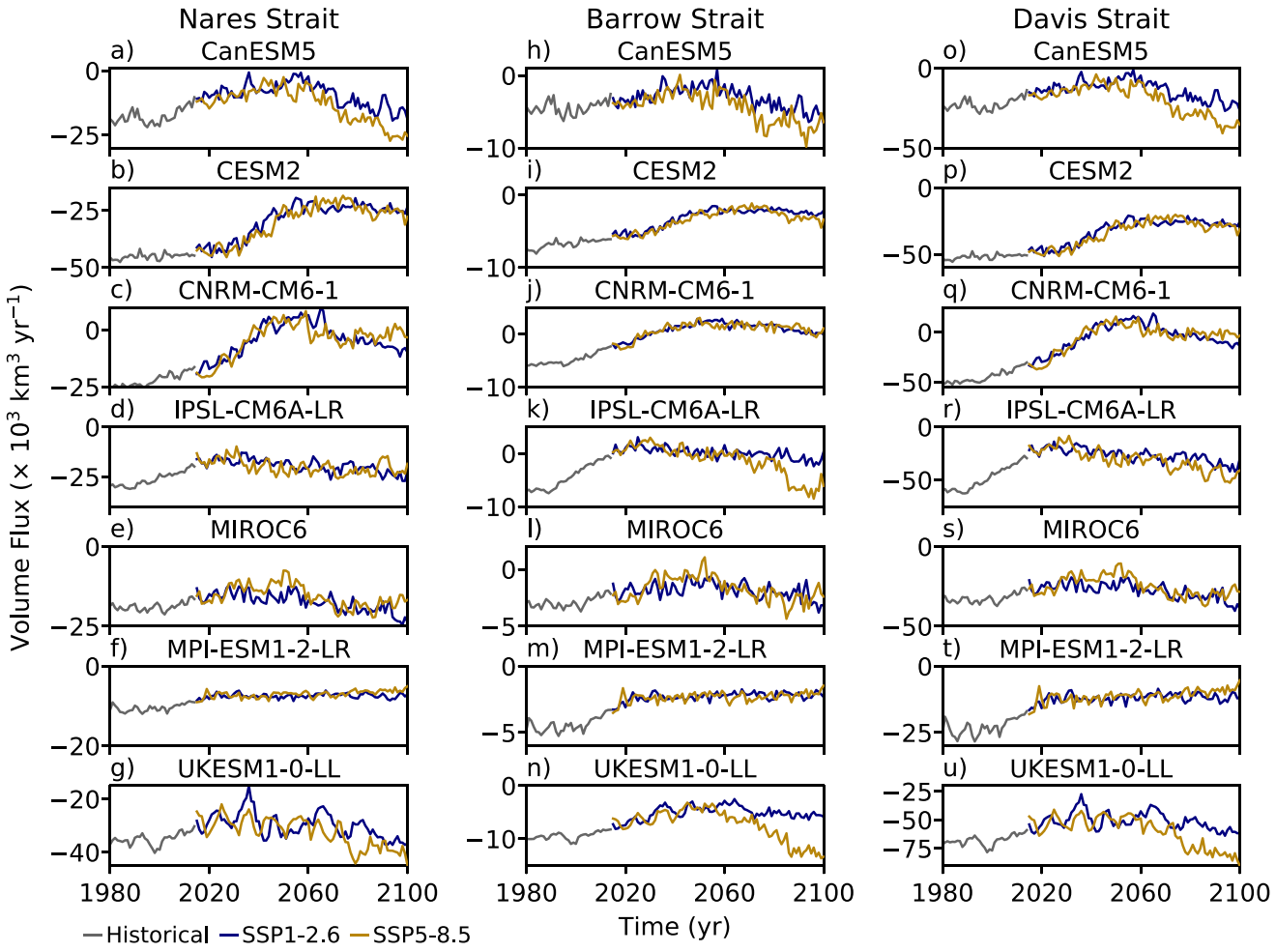

Figure 12. Ensemble mean volume fluxes ($\times 10^3$ km^3 yr^{-1}) for each model from 1980–2100 at (a–g) Nares Strait, (h–n) Barrow Strait, and (o–u) Davis Strait.

related is beyond the scope of this study. However, this is an important area of future work that may help address the prediction uncertainty in the 21st century evolution of the freshwater fluxes west of Greenland. In particular, an early-to-mid 21st century decrease in the freshwater flux west of Greenland in the CMIP6 models contrasts with the projected early emergence of positive trends in the Nares and Davis Strait liquid freshwater fluxes (Jahn & Laiho, 2020).

5. Conclusion

Using seven CMIP6 models, we compared 20th and 21st century Arctic freshwater storage and fluxes in the historical, and two future simulations, SSP1-2.6 and SSP5-8.5, to assess whether projections of these quantities have changed compared to previous CMIP models. We found that few models agreed well with 1980–2000 observations and that considerable intermodel differences existed across all simulations. By assessing models with 10 members or more, we showed that these differences cannot be explained by internal variability alone, as the spread from internal variability is consistently smaller than the intermodel spread. In agreement with studies using CMIP3 and CMIP5 models (e.g., Holland et al., 2006; Jahn & Holland, 2013; Jahn & Laiho, 2020; Shu et al., 2018), the seven models used here showed that late 21st century solid freshwater storage and export declines strongly due to Arctic sea ice loss, while liquid freshwater storage and export increases, albeit with large intermodel differences in the magnitude of these changes. Overall, this subset of CMIP6 models show a larger increase in the total freshwater export east of Greenland than west of Greenland in both SSP1-2.6 and SSP5-8.5.

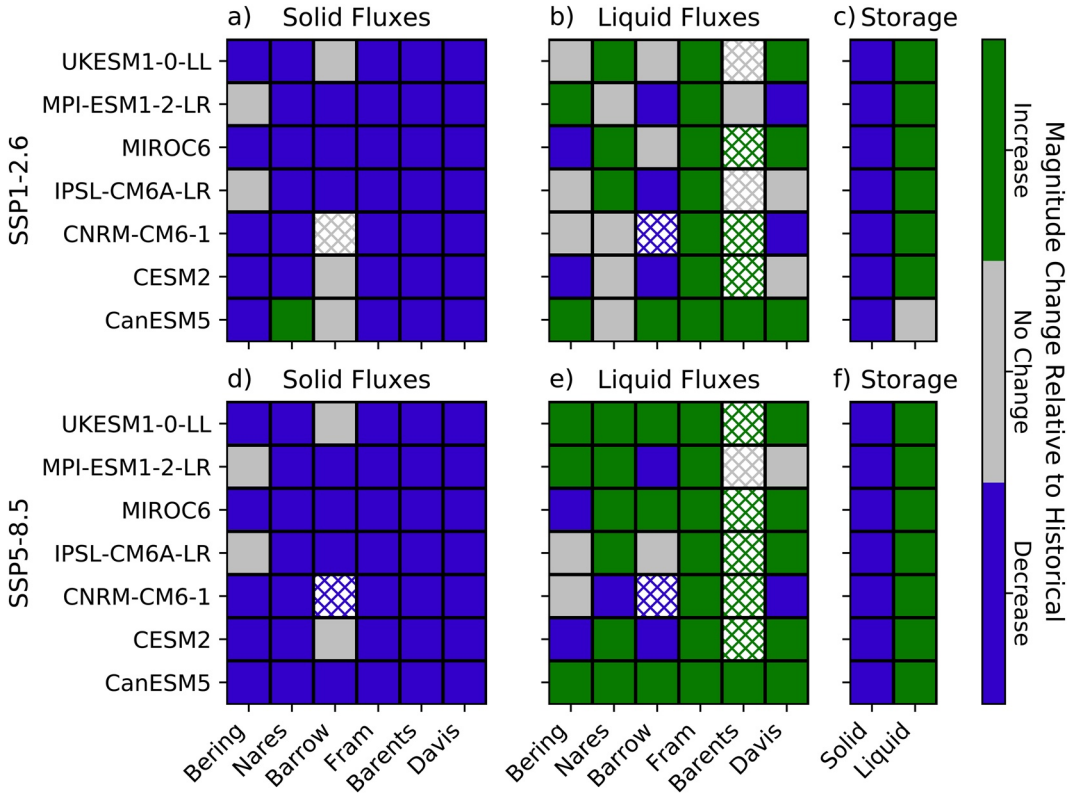

Figure 13. Qualitative model (a, d) solid flux, (b, e) liquid flux, and (c, f) storage changes in magnitude (absolute values of quantities) at the end of the 21st century (2080–2100 average) relative to the historical period (1980–2000 average) for (a–c) SSP1-2.6 and (d–f) SSP5-8.5. The threshold for change versus no change is set by the ±1 standard deviation error bars in Figures 6, 7, and 9. An overlap of the error bars in either future simulation compared to the historical simulation constitutes no change whereas no overlap constitutes a positive or negative change. Hatching indicates a sign change with the accompanying magnitude change given by the hatch color.

We also found that the models more consistently simulate salinity and volume flux anomalies compared to the oceanic freshwater fluxes that result from a combination of both. This corroborates the recent call by Schauer and Losch (2019) to analyze salinity and volume fluxes, as this provides more dynamical insight into the cause of the changes compared to freshwater fluxes. Model disagreement on the direction of the freshwater flux changes in Bering Strait and in the straits west of Greenland is ultimately determined by differences in the magnitude of the volume and salinity flux anomalies, but the models generally agree on the direction of their changes. When salinity and volume flux anomalies act in the same direction, or if one of them does not strongly contribute, we found the best intermodel agreement for projected changes in the liquid freshwater fluxes. Specifically, we showed that models agree best that the liquid freshwater export through Fram Strait will increase over the 21st century, and that volume and salinity flux changes contribute approximately equally to this increase. In the Barents Sea Opening, only salinity flux anomalies play a role, and all models agree that the reversal of the net liquid freshwater flux is due to these anomalies. In contrast, in the Bering Strait volume and salinity anomalies are of similar magnitude but oppose one another (the waters freshen but the volume flux decreases), with different magnitudes in different models that lead to projected small increases, small decreases, or steady Bering Strait liquid freshwater fluxes. The range of model disagreement is even larger west of Greenland, where models show stark differences in the projected changes in the liquid freshwater flux, particularly in the early 21st century, due to—yet again—opposing volume and salinity flux anomalies that have different magnitudes across models. While the models agree on a volume flux reduction in the early 21st century that reverses or stabilizes subsequently, they vary in the timing and magnitude of this change. Such an early 21st century decrease in the volume flux in the straits west of Greenland was not seen in CMIP5 and CMIP3 models (Holland et al., 2006; Shu et al., 2018), and it introduces new uncertainty into the projections of oceanic fluxes west of Greenland in this latest class of

models. Despite the model disagreement in the early-to-mid 21st century, by the end of the 21st century, the majority of models project an increase in the liquid freshwater export west of Greenland compared to the late 20th century due to a reversal of the volume flux anomaly and continued freshening.

Although broad agreement between the late 21st century changes among the models is encouraging, the persistence of large spreads in their historical storage and fluxes as well as in the magnitude of projected changes indicates that improvements in their Arctic Ocean simulations are still necessary. The persistence of these large intermodel disparities constitutes no fundamental improvement over CMIP5, although all models analyzed here now have two open gateways west of Greenland, allowing for a comparison of the Nares and Barrow Strait fluxes for the first time. Rectification of sea ice volume and ocean salinity biases, which (among other factors not considered in this study, such as the model resolution) directly influence model Arctic freshwater storage and fluxes, will likely improve intermodel agreement as well as agreement with observations. An important new issue found in the CMIP6 models is the disagreement among their late 20th to mid-21st century volume flux changes west of Greenland. Despite these issues, general projections of late 21st century Arctic freshwater storage and fluxes are robust across this subset of CMIP6 models and uphold the major results of previous CMIP generations.

Data Availability Statement

CMIP6 model output is available from the Earth System Grid Federation at https://esgf-node.llnl.gov/projects/cmip6/. Salinity data from the Polar Science Center Hydrographic Climatology 3.0 (PHC3.0) is available at http://psc.apl.washington.edu/nonwp_projects/PHC/Data3.html. Python was used for all analyses and for creating all figures. While this manuscript is under review, The timeseries of the Arctic Ocean freshwater terms calculated from the CMIP6 models is archived at the NSF Arctic Data Center (Zanowski and Jahn, 2021), and the code used to analyze the CMIP6 data is available on Zenodo (Zanowski 2021).

Acknowledgments
The authors thank Mitch Bushuk and Andrew Shao for providing details about specific models, advice on Arctic regridding, and general Arctic discussions as well as François Massonnet for discussions about the model-observation performance metric. We also acknowledge the high-performance computing support from Cheyenne (https://doi.org/10.5065/D6RX99HX) provided by NCAR's Computational and Information Systems Laboratory, sponsored by the National Science Foundation, and the data access and computing support provided by the NCAR CMIP Analysis Platform (https://doi.org/10.5065/D60R9MSP) that made this work possible, as well as the World Climate Research Programme, which, through its Working Group on Coupled Modeling, coordinated and promoted CMIP6. We thank the climate modeling groups for producing and making available their model output, the Earth System Grid Federation (ESGF) for archiving the data and providing access, and the multiple funding agencies who support CMIP6 and ESGF. This work was funded by the National Science Foundation under Award NSF-OPP 1504348, which supported the contributions by H. Zanowski and A. Jahn. M. M. Holland's contributions were supported by the National Center for Atmospheric Research (NCAR), which is a major facility sponsored by the NSF under Cooperative Agreement 1852977.

References

Aagaard, K., & Carmack, E. C. (1989). The role of sea ice and other fresh water in the Arctic circulation. *Journal of Geophysical Research*, *94*(C10), 14485–14498. https://doi.org/10.1029/JC094iC10p14485

Aksenov, Y., Bacon, S., Coward, A. C., & Holliday, N. P. (2010). Polar outflow from the Arctic Ocean: A high resolution model study. *Journal of Marine Systems*, *83*(1), 14–37. https://doi.org/10.1016/j.jmarsys.2010.06.007

Barton, B. I., Lenn, Y.-D., & Lique, C. (2018). Observed Atlantification of the Barents Sea causes the polar front to limit the expansion of winter sea ice. *Journal of Physical Oceanography*, *48*(8), 1849–1866. https://doi.org/10.1175/JPO-D-18-0003.1

Belkin, I. M., Levitus, S., Antonov, J., & Malmberg, S.-A. (1998). "Great Salinity Anomalies" in the North Atlantic. *Progress in Oceanography*, *41*(1), 1–68. https://doi.org/10.1016/s0079-6611(98)00015-9

Beszczynska-Möller, A., Woodgate, R. A., Lee, C. M., Melling, H., & Karcher, M. (2011). A synthesis of exchanges through the main oceanic gateways to the Arctic Ocean. *Oceanography*, *24*, 82–99. https://doi.org/10.5670/oceanog.2011.59

Biskaborn, B. K., Smith, S. L., Noetzli, J., Matthes, H., Vieira, G., Streletskiy, D. A., et al. (2019). Permafrost is warming at a global scale. *Nature Communications*, *10*, 264. https://doi.org/10.1038/s41467-018-08240-4

Boucher, O., Denvil, S., Levavasseur, G., Cozic, A., Caubel, A., Foujols, M.-A., et al. (2018). *IPSL IPSL-CM6A-LR model output prepared for CMIP6 CMIP historical. Version 20180803. Earth System Grid Federation*. https://doi.org/10.22033/ESGF/CMIP6.5195

Boucher, O., Denvil, S., Levavasseur, G., Cozic, A., Caubel, A., Foujols, M.-A., et al. (2019a). *IPSL IPSL-CM6A-LR model output prepared for CMIP6 ScenarioMIP ssp126. Version 20190903. Earth System Grid Federation*. https://doi.org/10.22033/ESGF/CMIP6.5262

Boucher, O., Denvil, S., Levavasseur, G., Cozic, A., Caubel, A., Foujols, M.-A., et al. (2019b). *IPSL IPSL-CM6A-LR model output prepared for CMIP6 ScenarioMIP ssp585. Version 20190903. Earth System Grid Federation*. https://doi.org/10.22033/ESGF/CMIP6.5271

Condron, A., Winsor, P., Hill, C., & Menemenlis, D. (2009). Simulated response of the Arctic freshwater budget to extreme NAO wind forcing. *Journal of Climate*, *22*(9), 2422–2437. https://doi.org/10.1175/2008JCLI2626.1

Cornish, S. B., Kostov, Y., Johnson, H. L., & Lique, C. (2020). Response of Arctic freshwater to the Arctic Oscillation in coupled climate models. *Journal of Climate*, *33*(7), 2533–2555. https://doi.org/10.1175/JCLI-D-19-0685.1

Curry, B., Lee, C. M., & Petrie, B. (2011). Volume, freshwater, and heat fluxes through Davis Strait, 2004-05*. *Journal of Physical Oceanography*, *41*(3), 429–436. https://doi.org/10.1175/2010JPO4536.1

Curry, B., Lee, C. M., Petrie, B., Moritz, R. E., & Kwok, R. (2014). Multiyear volume, liquid freshwater, and sea ice transports through Davis Strait, 2004-10*. *Journal of Physical Oceanography*, *44*(4), 1244–1266. https://doi.org/10.1175/JPO-D-13-0177.1

Danabasoglu, G. (2019a). *NCAR CESM2 model output prepared for CMIP6 CMIP historical. Version 20190308. Earth System Grid Federation*. https://doi.org/10.22033/ESGF/CMIP6.7627

Danabasoglu, G. (2019b). NCAR CESM2 model output prepared for CMIP6 ScenarioMIP ssp126. Version 20200528. *Earth System Grid Federation*. https://doi.org/10.22033/ESGF/CMIP6.7746

Danabasoglu, G. (2019c). NCAR CESM2 model output prepared for CMIP6 ScenarioMIP ssp585. Version 20200528. *Earth System Grid Federation*. https://doi.org/10.22033/ESGF/CMIP6.7768

de Steur, L., Hansen, E., Gerdes, R., Karcher, M., Fahrbach, E., & Holfort, J. (2009). Freshwater fluxes in the East Greenland Current: A decade of observations. *Geophysical Research Letters*, *36*(23), L23611. https://doi.org/10.1029/2009GL041278

de Steur, L., Peralta-Ferriz, C., & Pavlova, O. (2018). Freshwater export in the East Greenland Current freshens the North Atlantic. *Geophysical Research Letters*, *45*(24), 13359–13366. https://doi.org/10.1029/2018GL080207

Dickson, R. R., Meincke, J., Malmberg, S.-A., & Lee, A. J. (1988). The "great salinity anomaly" in the Northern North Atlantic 1968-1982. *Progress in Oceanography*, *20*(2), 103–151. https://doi.org/10.1016/0079-6611(88)90049-3

Eyring, V., Bony, S., Meehl, G. A., Senior, C. A., Stevens, B., Stouffer, R. J., & Taylor, K. E. (2016). Overview of the Coupled Model Intercomparison Project Phase 6 (CMIP6) experimental design and organization. *Geoscientific Model Development*, *9*(5), 1937–1958. https://doi.org/10.5194/gmd-9-1937-2016

Giles, K. A., Laxon, S. W., Ridout, A. L., Wingham, D. J., & Bacon, S. (2012). Western Arctic Ocean freshwater storage increased by wind-driven spin-up of the Beaufort Gyre. *Nature Geoscience*, *5*(3), 194–197. https://doi.org/10.1038/ngeo1379

Griffies, S. M., Biastoch, A., Böning, C., Bryan, F., Danabasoglu, G., Chassignet, E. P., et al. (2009). Coordinated Ocean-ice Reference Experiments (COREs). *Ocean Modelling*, *26*(1), 1–46. https://doi.org/10.1016/j.ocemod.2008.08.007

Haine, T. W. N., Curry, B., Gerdes, R., Hansen, E., Karcher, M., Lee, C., et al. (2015). Arctic freshwater export: Status, mechanisms, and prospects. *Global and Planetary Change*, *125*, 13–35. https://doi.org/10.1016/j.gloplacha.2014.11.013

Häkkinen, S., & Proshutinsky, A. (2004). Freshwater content variability in the Arctic Ocean. *Journal of Geophysical Research*, *109*, C03051. https://doi.org/10.1029/2003JC001940

Holland, M. M., Finnis, J., Barrett, A. P., & Serreze, M. C. (2007). Projected changes in Arctic Ocean freshwater budgets. *Journal of Geophysical Research*, *112*, G04S55. https://doi.org/10.1029/2006JG000354

Holland, M. M., Finnis, J., & Serreze, M. C. (2006). Simulated Arctic Ocean freshwater budgets in the twentieth and twenty-first centuries. *Journal of Climate*, *19*(23), 6221–6242. https://doi.org/10.1175/JCLI3967.1

Houssais, M.-N., & Herbaut, C. (2011). Atmospheric forcing on the Canadian Arctic Archipelago freshwater outflow and implications for the Labrador Sea variability. *Journal of Geophysical Research*, *116*, C00D02. https://doi.org/10.1029/2010JC006323

Hu, X., & Myers, P. G. (2014). Changes to the Canadian Arctic Archipelago Sea Ice and freshwater fluxes in the twenty-first century under the Intergovernmental Panel on Climate Change A1B climate scenario. *Atmosphere-Ocean*, *52*(4), 331–350. https://doi.org/10.1080/07055900.2014.942592

Jahn, A., Aksenov, Y., de Cuevas, B. A., de Steur, L., Häkkinen, S., Hansen, E., et al. (2012). Arctic Ocean freshwater: How robust are model simulations? *Journal of Geophysical Research*, *117*, C00D16. https://doi.org/10.1029/2012JC007907

Jahn, A., & Holland, M. M. (2013). Implications of Arctic sea ice changes for North Atlantic deep convection and the meridional overturning circulation in CCSM4-CMIP5 simulations. *Geophysical Research Letters*, *40*(6), 1206–1211. https://doi.org/10.1002/grl.50183

Jahn, A., & Laiho, R. (2020). Forced changes in the Arctic freshwater budget emerge in the early 21st century. *Geophysical Research Letters*, *47*(15), e2020GL088854. https://doi.org/10.1029/2020GL088854

Jahn, A., Tremblay, L. B., Newton, R., Holland, M. M., Mysak, L. A., & Dmitrenko, I. A. (2010). A tracer study of the Arctic Ocean's liquid freshwater export variability. *Journal of Geophysical Research*, *115*, C07015. https://doi.org/10.1029/2009JC005873

Kattsov, V. M., Walsh, J. E., Chapman, W. L., Govorkova, V. A., Pavlova, T. V., & Zhang, X. (2007). Simulation and projection of Arctic freshwater budget components by the IPCC AR4 global climate models. *Journal of Hydrometeorology*, *8*(3), 571–589. https://doi.org/10.1175/JHM575.1

Koenigk, T., Mikolajewicz, U., Haak, H., & Jungclaus, J. (2007). Arctic freshwater export in the 20th and 21st centuries. *Journal of Geophysical Research*, *112*, G04S41. https://doi.org/10.1029/2006JG000274

Lique, C., Holland, M. M., Dibike, Y. B., Lawrence, D. M., & Screen, J. A. (2016). Modeling the Arctic freshwater system and its integration in the global system: Lessons learned and future challenges. *Journal of Geophysical Research: Biogeosciences*, *121*(3), 540–566. https://doi.org/10.1002/2015JG003120

Münchow, A. (2016). Volume and freshwater flux observations from Nares Strait to the west of Greenland at daily time scales from 2003 to 2009. *Journal of Physical Oceanography*, *46*(1), 141–157. https://doi.org/10.1175/JPO-D-15-0093.1

McGeehan, T., & Maslowski, W. (2012). Evaluation and control mechanisms of volume and freshwater export through the Canadian Arctic Archipelago in a high-resolution pan-Arctic ice-ocean model. *Journal of Geophysical Research*, *117*, C00D14. https://doi.org/10.1029/2011JC007261

Meehl, G. A., Covey, C., Delworth, T., Latif, M., McAvaney, B., Mitchell, J. F. B., et al. (2007). The WCRP CMIP3 multimodel dataset: A new era in climate change research. *Bulletin of the American Meteorological Society*, *88*(9), 1383–1394. https://doi.org/10.1175/BAMS-88-9-1383

Nowicki, S., Goelzer, H., Seroussi, H., Payne, A. J., Lipscomb, W. H., Abe-Ouchi, A., et al. (2020). Experimental protocol for sea level projections from ISMIP6 stand-alone ice sheet models. *The Cryosphere*, *14*(7), 2331–2368. https://doi.org/10.5194/tc-14-2331-2020

O'Neill, B. C., Tebaldi, C., van Vuuren, D. P., Eyring, V., Friedlingstein, P., Hurtt, G., et al. (2016). The Scenario Model Intercomparison Project (ScenarioMIP) for CMIP6. *Geoscientific Model Development*, *9*(9), 3461–3482. https://doi.org/10.5194/gmd-9-3461-2016

Peterson, B. J., Holmes, R. M., McClelland, J. W., Vörösmarty, C. J., Lammers, R. B., Shiklomanov, A. I., et al. (2002). Increasing river discharge to the Arctic Ocean. *Science*, *298*(5601), 2171–2173. https://doi.org/10.1126/science.1077445

Peterson, B. J., McClelland, J., Curry, R., Holmes, R. M., Walsh, J. E., & Aagaard, K. (2006). Trajectory shifts in the Arctic and subarctic freshwater cycle. *Science*, *313*(5790), 1061–1066. https://doi.org/10.1126/science.1122593

Polyakov, I. V., Pnyushkov, A. V., Alkire, M. B., Ashik, I. M., Baumann, T. M., Carmack, E. C., et al. (2017). Greater role for Atlantic inflows on sea-ice loss in the Eurasian Basin of the Arctic Ocean. *Science*, *356*(6335), 285–291. https://doi.org/10.1126/science.aai8204

Prinsenberg, S. J., & Hamilton, J. (2005). Monitoring the volume, freshwater and heat fluxes passing through Lancaster Sound in the Canadian Arctic Archipelago. *Atmosphere-Ocean*, *43*(1), 1–22. https://doi.org/10.3137/ao.430101

Proshutinsky, A., Aksenov, Y., Clement Kinney, J., Gerdes, R., Golubeva, E., Holland, D., et al. (2011). Recent advances in Arctic Ocean studies employing models from the Arctic Ocean Model Intercomparison Project. *Oceanography*, *24*, 102. https://doi.org/10.5670/oceanog.2011.61

Proshutinsky, A., Krishfield, R., Timmermans, M.-L., Toole, J., Carmack, E., McLaughlin, F., et al. (2009). Beaufort Gyre freshwater reservoir: State and variability from observations. *Journal of Geophysical Research*, *114*, C00A10. https://doi.org/10.1029/2008JC005104

Proshutinsky, A., Steele, M., & Timmermans, M.-L. (2016). Forum for Arctic Modeling and Observational Synthesis (FAMOS): Past, current, and future activities. *Journal of Geophysical Research: Oceans*, *121*(6), 3803–3819. https://doi.org/10.1002/2016JC011898

Prowse, T., Bring, A., Mård, J., Carmack, E., Holland, M., Instanes, A., et al. (2015). Arctic freshwater synthesis: Summary of key emerging issues. *Journal of Geophysical Research: Biogeosciences*, *120*(10), 1887–1893. https://doi.org/10.1002/2015JG003128

Rabe, B., Karcher, M., Kauker, F., Schauer, U., Toole, J. M., Krishfield, R. A., et al. (2014). Arctic Ocean basin liquid freshwater storage trend 1992-2012. *Geophysical Research Letters*, *41*(3), 961–968. https://doi.org/10.1002/2013GL058121

Rabe, B., Karcher, M., Schauer, U., Toole, J. M., Krishfield, R. A., Pisarev, S., et al. (2011). An assessment of Arctic Ocean freshwater content changes from the 1990s to the 2006-2008 period. *Deep Sea Research I: Oceanographic Research Papers*, *58*(2), 173–185. https://doi.org/10.1016/j.dsr.2010.12.002

Rawlins, M. A., Steele, M., Holland, M. M., Adam, J. C., Cherry, J. E., Francis, J. A., et al. (2010). Analysis of the Arctic system for freshwater cycle intensification: Observations and expectations. *Journal of Climate*, *23*(21), 5715–5737. https://doi.org/10.1175/2010JCLI3421.1

Rowland, J. C., Jones, C. E., Altmann, G., Bryan, R., Crosby, B. T., Hinzman, L. D., et al. (2010). Arctic landscapes in transition: Responses to thawing permafrost. *Eos*, *91*(26), 229–230. https://doi.org/10.1029/2010EO260001

Saenko, O. A., Yang, D., & Myers, P. G. (2017). Response of the North Atlantic dynamic sea level and circulation to Greenland meltwater and climate change in an eddy-permitting ocean model. *Climate Dynamics*, *49*(7), 2895–2910. https://doi.org/10.1007/s00382-016-3495-7

Schauer, U., & Losch, M. (2019). "Freshwater" in the ocean is not a useful parameter in climate research. *Journal of Physical Oceanography*, *49*(9), 2309–2321. https://doi.org/10.1175/JPO-D-19-0102.1

Serreze, M. C., Barrett, A. P., Slater, A. G., Woodgate, R. A., Aagaard, K., Lammers, R. B., et al. (2006). The large-scale freshwater cycle of the Arctic. *Journal of Geophysical Research*, *111*, C11010. https://doi.org/10.1029/2005JC003424

Sévellec, F., Fedorov, A. V., & Liu, W. (2017). Arctic sea-ice decline weakens the Atlantic Meridional Overturning Circulation. *Nature Climate Change*, *7*(8), 604–610. https://doi.org/10.1038/nclimate3353

Shepherd, A., Ivins, E., Rignot, E., Smith, B., van den Broeke, M., Velicogna, I., et al. (2020). Mass balance of the Greenland Ice Sheet from 1992 to 2018. *Nature*, *579*(7798), 233–239. https://doi.org/10.1038/s41586-019-1855-2

Shu, Q., Qiao, F., Song, Z., Zhao, J., & Li, X. (2018). Projected freshening of the Arctic Ocean in the 21st century. *Journal of Geophysical Research: Oceans*, *123*(12), 9232–9244. https://doi.org/10.1029/2018JC014036

Shu, Q., Song, Z., & Qiao, F. (2015). Assessment of sea ice simulations in the CMIP5 models. *The Cryosphere*, *9*(1), 399–409. https://doi.org/10.5194/tc-9-399-2015

Steele, M., Morley, R., & Ermold, W. (2001). PHC: A global ocean hydrography with a high-quality Arctic Ocean. *Journal of Climate*, *14*(9), 2079–2087. https://doi.org/10.1175/1520-0442(2001)014⟨2079:PAGOHW⟩2.0.CO;2

Stroeve, J. C., Holland, M. M., Meier, W., Scambos, T., & Serreze, M. (2007). Arctic sea ice decline: Faster than forecast. *Geophysical Research Letters*, *34*, L09501. https://doi.org/10.1029/2007GL029703

Stroeve, J. C., Serreze, M. C., Holland, M., Kay, J. E., Malanik, J., & Barrett, A. P. (2012). The Arctic's rapidly shrinking sea ice cover: A research synthesis. *Climate Change*, *110*(3), 1005–1027. https://doi.org/10.1007/s10584-011-0101-1

Swart, N. C., Cole, J. N., Kharin, V. V., Lazare, M., Scinocca, J. F., Gillett, N. P., et al. (2019a). CCCma CanESM5 model output prepared for CMIP6 CMIP historical. Version 20190429. *Earth System Grid Federation*. https://doi.org/10.22033/ESGF/CMIP6.3610

Swart, N. C., Cole, J. N., Kharin, V. V., Lazare, M., Scinocca, J. F., Gillett, N. P., et al. (2019b). CCCma CanESM5 model output prepared for CMIP6 ScenarioMIP ssp126. Version 20190429. *Earth System Grid Federation*. https://doi.org/10.22033/ESGF/CMIP6.10269

Swart, N. C., Cole, J. N., Kharin, V. V., Lazare, M., Scinocca, J. F., Gillett, N. P., et al. (2019c). CCCma CanESM5 model output prepared for CMIP6 ScenarioMIP ssp585. Version 20190429. *Earth System Grid Federation*. https://doi.org/10.22033/ESGF/CMIP6.3696

Tang, Y., Rumbold, S., Ellis, R., Kelley, D., Mulcahy, J., Sellar, A., et al. (2019a). MOHC UKESM1.0-LL model output prepared for CMIP6 CMIP historical. Version 20190627. *Earth System Grid Federation*. https://doi.org/10.22033/ESGF/CMIP6.6113

Tang, Y., Rumbold, S., Ellis, R., Kelley, D., Mulcahy, J., Sellar, A., et al. (2019b). MOHC UKESM1.0-LL model output prepared for CMIP6 ScenarioMIP ssp126. Version 20190708. *Earth System Grid Federation*. https://doi.org/10.22033/ESGF/CMIP6.6333

Tang, Y., Rumbold, S., Ellis, R., Kelley, D., Mulcahy, J., Sellar, A., et al. (2019c). MOHC UKESM1.0-LL model output prepared for CMIP6 ScenarioMIP ssp585. Version 20190726. *Earth System Grid Federation*. https://doi.org/10.22033/ESGF/CMIP6.6405

Tatebe, H., & Watanabe, M. (2018). MIROC MIROC6 model output prepared for CMIP6 CMIP historical. Version 20190311. *Earth System Grid Federation*. https://doi.org/10.22033/ESGF/CMIP6.5603

Tatebe, H., & Watanabe, M. (2019a). MIROC MIROC6 model output prepared for CMIP6 ScenarioMIP ssp126. Version 20190627. *Earth System Grid Federation*. https://doi.org/10.22033/ESGF/CMIP6.5743

Tatebe, H., & Watanabe, M. (2019b). MIROC MIROC6 model output prepared for CMIP6 ScenarioMIP ssp585. Version 20190627. *Earth System Grid Federation*. https://doi.org/10.22033/ESGF/CMIP6.5771

Taylor, K. E., Stouffer, R. J., & Meehl, G. A. (2012). An overview of CMIP5 and the experiment design. *Bulletin of the American Meteorological Society*, *93*(4), 485–498. https://doi.org/10.1175/BAMS-D-11-00094.1

Thornalley, D. J. R., Oppo, D. W., Ortega, P., Robson, J. I., Brierley, C. M., Davis, R., et al. (2018). Anomalously weak Labrador Sea convection and Atlantic overturning during the past 150 years. *Nature*, *556*(7700), 227–230. https://doi.org/10.1038/s41586-018-0007-4

Vavrus, S. J., Holland, M. M., Jahn, A., Bailey, D. A., & Blazey, B. A. (2012). Twenty-first-century Arctic climate change in CCSM4. *Journal of Climate*, *25*(8), 2696–2710. https://doi.org/10.1175/JCLI-D-11-00220.1

Voldoire, A. (2018). CMIP6 Simulations of the CNRM-CERFACS based on CNRM-CM6-1 model for CMIP experiment historical. Version 20180917. *Earth System Grid Federation*. https://doi.org/10.22033/ESGF/CMIP6.4066

Voldoire, A. (2019a). CNRM-CERFACS CNRM-CM6-1 model output prepared for CMIP6 ScenarioMIP ssp126. Version 20190219. *Earth System Grid Federation*. https://doi.org/10.22033/ESGF/CMIP6.4184

Voldoire, A. (2019b). CNRM-CERFACS CNRM-CM6-1 model output prepared for CMIP6 ScenarioMIP ssp585. Version 20190219. *Earth System Grid Federation*. https://doi.org/10.22033/ESGF/CMIP6.4224

Wang, Q., Ilicak, M., Gerdes, R., Drange, H., Aksenov, Y., Bailey, D. A., et al. (2016a). An assessment of the Arctic Ocean in a suite of interannual CORE-II simulations. Part II: Liquid freshwater. *Ocean Modelling*, *99*, 86–109. https://doi.org/10.1016/j.ocemod.2015.12.009

Wang, Q., Ilicak, M., Gerdes, R., Drange, H., Aksenov, Y., Bailey, D. A., et al. (2016b). An assessment of the Arctic Ocean in a suite of interannual CORE-II simulations. Part I: Sea ice and solid freshwater. *Ocean Modelling*, *99*, 110–132. https://doi.org/10.1016/j.ocemod.2015.12.008

Wang, Q., Wekerle, C., Danilov, S., Koldunov, N., Sidorenko, D., Sein, D., et al. (2018). Arctic sea ice decline significantly contributed to the unprecedented liquid freshwater accumulation in the Beaufort Gyre of the Arctic Ocean. *Geophysical Research Letters*, *45*(10), 4956–4964. https://doi.org/10.1029/2018GL077901

Wang, Q., Wekerle, C., Danilov, S., Sidorenko, D., Koldunov, N., Sein, D., et al. (2019). Recent sea ice decline did not significantly increase the total liquid freshwater content of the Arctic Ocean. *Journal of Climate*, *32*(1), 15–32. https://doi.org/10.1175/JCLI-D-18-0237.1

Weijer, W., Cheng, W., Garuba, O. A., Hu, A., & Nadiga, B. T. (2020). CMIP6 models predict significant 21st century decline of the Atlantic Meridional Overturning Circulation. *Geophysical Research Letters*, *47*(12), e2019GL086075. https://doi.org/10.1029/2019GL086075

Wieners, K.-H., Giorgetta, M., Jungclaus, J., Reick, C., Esch, M., Bittner, M., et al. (2019a). MPI-M MPI-ESM1.2-LR model output prepared for CMIP6 CMIP historical. Version 20190710. *Earth System Grid Federation*. https://doi.org/10.22033/ESGF/CMIP6.6595

Wieners, K.-H., Giorgetta, M., Jungclaus, J., Reick, C., Esch, M., Bittner, M., et al. (2019b). MPI-M MPI-ESM1.2-LR model output prepared for CMIP6 ScenarioMIP ssp126. Version 20190710. *Earth System Grid Federation*. https://doi.org/10.22033/ESGF/CMIP6.6690

Wieners, K.-H., Giorgetta, M., Jungclaus, J., Reick, C., Esch, M., Bittner, M., et al. (2019c). MPI-M MPI-ESM1.2-LR model output prepared for CMIP6 ScenarioMIP ssp585. Version 20190710. *Earth System Grid Federation*. https://doi.org/10.22033/ESGF/CMIP6.6705

Woodgate, R. A. (2018). Increases in the Pacific inflow to the Arctic from 1990 to 2015, and insights into seasonal trends and driving mechanisms from year-round Bering Strait mooring data. *Progress in Oceanography*, *160*, 124–154. https://doi.org/10.1016/j.pocean.2017.12.007

Woodgate, R. A., Weingartner, T. J., & Lindsay, R. (2012). Observed increases in Bering Strait oceanic fluxes from the Pacific to the Arctic from 2001 to 2011 and their impacts on the Arctic Ocean water column. *Geophysical Research Letters*, *39*, L24603. https://doi.org/10.1029/2012GL054092

Yang, Q., Dixon, T. H., Myers, P. G., Bonin, J., Chambers, D., van den Broeke, M. R., et al. (2016). Recent increases in Arctic freshwater flux affects Labrador Sea convection and Atlantic overturning circulation. *Nature Communications*, *7*, 10525. https://doi.org/10.1038/ncomms10525

Zanowski, H. (2021). *HannahZanowski/CMIP6_ArcticFW: Arctic FW Storage and Fluxes in CMIP6 Models (Version v1.0.0)*, Zenodo. https://doi.org/10.5281/zenodo.4606856

Zanowski, H., & Jahn, A. (2021). *Arctic Ocean freshwater storage and fluxes from CMIP6 model ensembles 1950-2100*, Arctic Data Center. https://doi.org/10.18739/A2154DQ22